Available online at www.sciencedirect.com
ScienceDirect
Journal of Computational Physics 218 (2006) 720–747
JOURNAL OF COMPUTATIONAL PHYSICS
www.elsevier.com/locate/jcp

A variational hexahedral grid generator with control metric

Boris N. Azarenok

Dorodnicyn Computing Center of the Russian Academy of Sciences, Vavilov Str. 40, GSP-1, Moscow 119991, Russia

Received 20 August 2005; received in revised form 3 March 2006; accepted 6 March 2006
Available online 21 April 2006

Abstract

A variational method of constructing a spatial structured grid composed of hexahedral cells is presented. The method executes a minimization of the variational functional. The integrand of the functional is a ratio of the orthogonal invariants. The functional depends on two metrics. One metric is induced by a curvilinear mesh generated in the physical domain and the other control metric, given in the canonical domain, is responsible for an additional cell shape control, for instance, for condensing the coordinate surfaces and orthogonalization of the grid lines towards the domain boundary. Generally, defining the control metric allows to generate an arbitrary given non-folded mesh in the physical domain. For every cell, the functional is discretized on ten tetrahedra forming two dodecahedrons with the same vertices which span the hexahedral cell. The discrete functional possesses an infinite barrier on the boundary of the set of non-folded dodecahedral cells that ensures the construction of the non-folded grid composed of such cells. In the most practical cases the hexahedral grid with the same nodes is non-folded as well. The method of boundary nodes redistribution is considered. Examples of the grid construction are reported.

Keywords: Structured hexahedral mesh; Minimization of functional; Infinite barrier; Control metric

1. Introduction

The first variational grid generation methods were suggested for the one-dimensional case in [1] and for the two-dimensional one in [2,3]. Henceforth, the developing of various functionals was performed with purpose to construct non-folded meshes and to execute an additional control for the coordinate lines, see [4–16]. The problem of generating non-folded meshes, composed of quadrilateral cells, in an arbitrary 2D domain was solved in [9] where the variational barrier method was developed. In [17], it is used a functional being the combination of the terms being responsible for the mesh uniformity and orthogonality. In [3,4], the second control metric in the parametric domain was introduced with purpose to include an additional control for grid lines behavior and the algorithm of the quasi-orthogonal mesh construction was suggested. In [18,19], the superposition of the quasi-isometric and conformal mappings was considered. In [20], the composition of the grid control map and the inverse of the harmonic map was applied. In [6], the functional that measures a grid

E-mail address: azarenok@ccas.ru.

0021-9991/$ - see front matter
doi:10.1016/j.jcp.2006.03.004

smoothness was considered and applied jointly with the functionals of orthogonality and adaptivity. Other type functionals (length, uniformity, etc.) are reported, for instance, in [7,12–14]. In [21] (see also [22]), it was suggested an universal functional describing all classes of invertible discrete transformations of the 2D parametric domain to the physical one.

The 3D case turned out much harder than 2D. First, it concerns with the search of a transformation providing a homeomorphic mapping of the unit parametric cube onto an arbitrary domain. For instance, it is unknown yet whether a harmonic mapping (well-studied for 2D transformations, see, e.g. [23]) of an arbitrary domain onto a convex domain (unit cube) with a given one-to-one mapping between the boundaries is always a homeomorphism. There is an example (see [24]) when, subject to some conditions imposed on the boundaries, the harmonic mapping is not a homeomorphism. A study on seeking conditions providing the mapping is a global homeomorphism was executed in [25–27]. Second, for a hexahedral cell (also called a ruled cell) with ruled faces there is no a condition, being simultaneously a necessary and sufficient one, providing non-degeneracy of the cell [28,29]. In [30], the method of the 3D adaptive moving mesh construction was developed when it is minimized the dimensional functional of smoothness suggested in [11]. In [31], it is considered the method based on optimization of an objective function, being the shape-quality measure for hexahedral elements, which is used to built unstructured hexahedral meshes. In [32,33], hexahedral grids are constructed by minimizing the functional being the sum of the uniformity and orthogonality functionals.

When constructing spatial meshes, the problem of additional control for coordinate surfaces is of particular importance. Modeling of the aerodynamical problems requires to condense the coordinate surfaces and orthogonalize the coordinate lines towards the domain boundary to resolve the boundary layers. When calculating the problems with an unstable interphase boundary of two media, its shape bends significantly and it is not easy to generate the mesh in subdomains of instability. There is a need to extend the mesh control methods, developed for the 2D problems, to the spatial case. The idea of using the second control metric with this purpose was proposed in [34].

In the paper, we apply the idea of using the control metric of [34] for a variational method of constructing a spatial structured grid composed of hexahedral cells. In the method a variational functional is minimized. The integrand of the functional is a ratio of the orthogonal invariants. The functional depends on two metrics. One metric is induced by a curvilinear mesh generated in the physical domain and the other control metric, given in the canonical domain, is responsible for an additional cell shape control. Generally, defining the control metric allows to generate an arbitrary given non-folded mesh in the physical domain.

The outline of the paper is as follows: Section 2 gives the derivation of the functional and two formulations of the variational problem of the grid construction. Section 3 presents the property of the 3D functional to attain an absolute minimum for a given mesh and the Euler–Lagrange equations for the functional are considered. Section 4 discusses non-degeneracy conditions for a hexahedral cell. It is expressed an idea to substitute a ruled cell for two dodecahedrons, each consists of five tetrahedra, and to apply the non-degeneracy condition for the 10 tetrahedra. Section 5 discusses the way of discretizing the functional. The minimizing procedure for the discrete functional is described in Section 6 and computational formulae are given in Section 7. In Section 8, the barrier property of the discrete functional is discussed. The method of boundary nodes redistribution is presented in Section 9. Section 10 describes the way of condensing the coordinate surfaces and orthogonalizing the grid lines towards the boundary. Section 11 presents the algorithm of obtaining an initial non-folded mesh. Two examples of the grid construction are reported in Section 12. Section 13 discusses other functionals.

2. Variational functional

We give a derivation of the functional using the idea of [34]. Consider a smooth invertible mapping $\mathbf{x}(\mathbf{X}) : \mathbb{R}^n \to \mathbb{R}^n$ of the canonical domain in space of variables $\mathbf{X} = (X^1, \ldots, X^n)$ to the physical domain in space of variables $\mathbf{x} = (x^1, \ldots, x^n)$ with the Jacobian matrix $a^i_j = \partial x^i / \partial X^j$. Consider also two auxiliary smooth invertible mappings $\mathbf{x}(\boldsymbol{\xi}), \mathbf{X}(\boldsymbol{\xi}) : \mathbb{R}^n \to \mathbb{R}^n$ of the parametric domain, the unit cube $0 \leqslant \xi^1, \ldots, \xi^n \leqslant 1$, in space of variables $\boldsymbol{\xi} = (\xi^1, \ldots, \xi^n)$ to the physical and canonical domains, respectively, with the Jacobian matrices $b^i_j = \partial x^i / \partial \xi^j$ and $c^i_j = \partial X^i / \partial \xi^j$ (see Fig. 1 for the case $n = 3$).

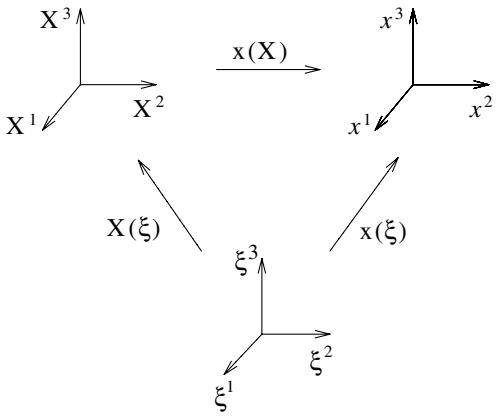

Fig. 1. Spatial case $n = 3$.

The mappings induce the metric tensors h, g, G which read

$$h = a^{\top}a, \quad g = b^{\top}b, \quad G = c^{\top}c,$$

where $a^{\top}$, $b^{\top}$, and $c^{\top}$ are the transposed matrices. Since $b = ac$ and, therefore, $a = bc^{-1}$, we have for the metric h

$$h = a^{\top}a = (c^{-1})^{\top}b^{\top}bc^{-1}.$$

Let us write the characteristic equation for the metric h

$$\det(h - \lambda\mathscr{I}) = 0,$$

where $\mathscr{I}$ is the identity matrix. Substitution of h expressed in terms of the matrices b, c yields

$$\det(b^{\top}b - \lambda c^{\top}c) = 0$$

or in terms of the metrics g, G

$$\det(g - \lambda G) = \det G \det(G^{-1}g - \lambda\mathscr{I}) = 0.$$

The mapping $\mathbf{X}(\boldsymbol{\xi})$ is invertible, therefore, $\det G \neq 0$ and the matrix equation for determining the eigenvalues λ_i, $i = 1,\ldots,n$, takes the form

$$\det(G^{-1}g - \lambda\mathscr{I}) = 0.$$

It can be rewritten as

$$\lambda^n + I_1\lambda^{n-1} + \cdots + I_n = 0. \tag{1}$$

The matrix $G^{-1}g$ is symmetric and positive definite, therefore, the algebraic equation (1) has n real roots $\lambda_i > 0$. The coefficients $I_1,\ldots,I_n$ are known as the orthogonal invariants of the metric h because they do not change under orthogonal transformations of the coordinate system. In particular

$$I_1 = \operatorname{tr}(G^{-1}g) = \sum_{i=1}^{n} h_{ii} = \sum_{i=1}^{n} \lambda_i, \quad I_n = \det(G^{-1}g) = \lambda_1 \ldots \lambda_n. \tag{2}$$

The function of the invariants I_i is also an invariant.

We will use two formulations of the variational problem of the grid construction.

Formulation 1. The grid construction problem is considered as a discrete implementation of a smooth one-to-one mapping $\mathbf{x}(\mathbf{X}) : \mathbb{R}^n \to \mathbb{R}^n$ of the canonical domain to the physical domain provided that the boundary correspondence is given. To this end, one minimizes a functional being the integral of a function depending on the metric invariants.

Consider the ratio of the invariant I_1 to I_n raised to proper power so as to obtain a non-dimensional function

$$E = \frac{1}{n^{n/2}}\frac{I_1^{n/2}}{I_n^{1/2}} = \frac{1}{n^{n/2}}\frac{(\operatorname{tr}(G^{-1}g))^{n/2}}{\sqrt{\det(G^{-1}g)}} = \frac{1}{n^{n/2}}\frac{(\operatorname{tr}(G^{-1}g))^{n/2}\sqrt{\det G}}{\sqrt{\det g}}. \tag{3}$$

It is easily seen that the function E is invariant to invertible orthogonal transformations and homothetic dilatation of the coordinate systems $\mathbf{x}$ and $\mathbf{X}$. The meaning of the normalization factor $n^{-n/2}$ will be clarified in Section 3. The idea of using the invariant-to-invariant ratio in constructing the functionals was proposed in [11].

Consider the following functional for the invariant E, being the integral over the n-dimensional unit cube, [34]

$$\mathscr{D}(\mathbf{x}(\boldsymbol{\xi})) = \int_0^1 E\,\mathrm{d}\xi^1 \cdots \mathrm{d}\xi^n = \frac{1}{n^{n/2}} \int_0^1 \frac{(\mathrm{tr}(G^{-1}g))^{n/2}\sqrt{\det G}}{\sqrt{\det g}}\,\mathrm{d}\xi^1 \cdots \mathrm{d}\xi^n. \tag{4}$$

In [34], this functional was derived by using the conformal invariants. The functional (4) is the invariant to the above transformations of the coordinates $\mathbf{x}$ and $\mathbf{X}$. But (4) is not an invariant to dilatation of the coordinates $\boldsymbol{\xi}$ due to emerging the Jacobian of transformation $(\det \tilde{g})^{1/2}$. Note that similar functionals were applied in [8,11].

In the case of $n = 2$, when the metric G is Euclidian ($G_{ij} = \delta_{ij}$, where δ_{ij} is the Kronecker delta) and $\mathbf{x} = (x, y)$, $\boldsymbol{\xi} = (\xi, \eta)$, (4) turns into the functional of smoothness proposed in [6](see also [7,12,13])

$$\mathscr{D} = \frac{1}{2}\int_0^1 \frac{x_\xi^2 + y_\xi^2 + x_\eta^2 + y_\eta^2}{x_\xi y_\eta - x_\eta y_\xi}\mathrm{d}\xi\,\mathrm{d}\eta. \tag{5}$$

When G is the Riemannian metric, from (4) one obtains the functional [21]

$$\mathscr{D} = \frac{1}{2}\int_0^1 \frac{x_\xi^2 G_{22} - 2x_\xi x_\eta G_{12} + x_\eta^2 G_{11} + y_\xi^2 G_{22} - 2y_\xi y_\eta G_{12} + y_\eta^2 G_{11}}{(x_\xi y_\eta - x_\eta y_\xi)\sqrt{G_{11}G_{22} - G_{12}^2}}\,\mathrm{d}\xi\,\mathrm{d}\eta \tag{6}$$

and the function E is called the energy density of the mapping. If in the denominator of (6) to remove the Jacobian $x_\xi y_\eta - x_\eta y_\xi$, we get the functional suggested in [3].

The formulation 1 is applied to derive the variational functional (4). In practical implementation, sometimes it is convenient to use one more variational formulation.

Formulation 2. It is required to find a smooth one-to-one mapping $\mathbf{x}(\boldsymbol{\xi}) : \mathbb{R}^n \to \mathbb{R}^n$ of the parametric domain (unit cube) to the physical domain provided that the boundary correspondence is given. The functions $\mathbf{x}(\boldsymbol{\xi})$, executing the mapping, are sought while minimizing the functional (4). Here $G_{ij}(\boldsymbol{\xi})$ are the elements of a symmetric positive definite matrix given at every point of the parametric cube.

As well as in the formulation 1 we introduce the second parametrization, i.e., dependence $\mathbf{X}(\boldsymbol{\xi})$. However, we need not consider the mapping of the canonical domain. For instance, the metric elements G_{ij} may be defined via the transformation of a cell in parametric space to the given cell in space $\mathbf{X}$. Meantime it does not matter what it is a union of all cells in $\mathbf{X}$. In 2D, such a formulation was applied in [21,22]. Another way is to specify directly the metric elements G_{ij} imposing some conditions on the mesh, see [5,35,36].

3. Property of 3D functional and Euler–Lagrange equations

In the spatial case $n = 3$ with coordinates $\mathbf{x} = (x, y, z)$, $\mathbf{X} = (X, Y, Z)$, $\boldsymbol{\xi} = (\xi, \eta, \zeta)$, the functional (4) reads

$$\mathscr{D} = \int_0^1 E\,\mathrm{d}\xi\,\mathrm{d}\eta\,\mathrm{d}\zeta = \frac{1}{3^{3/2}}\int_0^1 \frac{(\mathrm{tr}(G^{-1}g))^{3/2}\sqrt{\det G}}{\sqrt{\det g}}\,\mathrm{d}\xi\,\mathrm{d}\eta\,\mathrm{d}\zeta. \tag{7}$$

Here

$$\mathrm{tr}(G^{-1}g) = G^{ij}g_{ji} = G^{11}g_{11} + G^{22}g_{22} + G^{33}g_{33} + 2G^{12}g_{12} + 2G^{13}g_{13} + 2G^{23}g_{23},$$

G^{ij} are the elements of the inverse matrix G^{-1} (contravariant tensor) and the standard summation convention is applied. At a point in space $\mathbf{x}$ with the coordinates $\mathbf{r} = (x, y, z)$, the elements of the metric tensor g are

$$g_{11} = \mathbf{r}_\xi^2, \quad g_{22} = \mathbf{r}_\eta^2, \quad g_{33} = \mathbf{r}_\zeta^2, \quad g_{12} = (\mathbf{r}_\xi \cdot \mathbf{r}_\eta), \quad g_{13} = (\mathbf{r}_\xi \cdot \mathbf{r}_\zeta), \quad g_{23} = (\mathbf{r}_\eta \cdot \mathbf{r}_\zeta) \tag{8}$$

and the elements of the metric tensor G at a point in space $\mathbf{X}$ with the coordinates $\tilde{\mathbf{r}} = (X, Y, Z)$ are defined analogously.

Recalling (2) we rewrite (3) in terms of the eigenvalues of the matrix $G^{-1}g$

$$E(\lambda_1,\lambda_2,\lambda_3)=\frac{1}{3^{3/2}}\frac{(\lambda_1+\lambda_2+\lambda_3)^{3/2}}{\sqrt{\lambda_1\lambda_2\lambda_3}}.$$

Taking into account the general inequality for the arithmetic mean and geometric mean of arbitrary positive numbers $q_1,\ldots,q_n$

$$\frac{1}{n}\sum_{i=1}^{n}q_i\geqslant\left(\prod_{i=1}^{n}q_i\right)^{1/n}$$

and substituting λ_i in it (recall that all $\lambda_i>0$), we obtain

$$\frac{1}{3}(\lambda_1+\lambda_2+\lambda_3)\geqslant\sqrt[3]{\lambda_1\lambda_2\lambda_3}$$

and immediately get that $E\geqslant 1$. The necessary condition for a minimum of E to attain is

$$\frac{\partial E}{\partial\lambda_i}=0,\quad i=1,2,3.$$

Differentiating E yields three relations with respect to λ_i

$$2\lambda_1-\lambda_2-\lambda_3=0,\quad 2\lambda_2-\lambda_1-\lambda_3=0,\quad 2\lambda_3-\lambda_1-\lambda_2=0.$$

Combining by pairs these relations, we find that the minimum of E is attained subject to $\lambda_1=\lambda_2=\lambda_3$ and its value is $E_{\min}=1$. Now it is seen why the normalization factor in (3) is defined equal $n^{-n/2}$.

Let a smooth invertible mapping $\mathbf{x}(\boldsymbol{\xi})$ with the metric g be given. Defining $G=g$ at every point of the parametric cube, in (7) we have that the function $E\equiv 1$. Hence, the absolute minimum of the functional $\mathscr{D}$ equal 1 is attained. We conclude that an arbitrary smooth invertible mapping $\mathbf{x}(\boldsymbol{\xi})$ may be produced by minimizing the functional (7) with a given metric G. Thus, defining the control metric G allows to control the metric g or, in other words, to govern the coordinate surfaces in the physical domain. That is why, the functional (7) may be called universal by analogy with the term used in [35] with respect to the functional of [3] and (6).

The functional (7) is non-convex and in domains of complicated geometry there can be several stationary points when the absolute minimum of the functional is not attained. The non-uniqueness of the solution of the minimization problem for the functionals (5) and (6) was discussed in [35,37].

The Euler–Lagrange equations for (7) are the system of nonlinear differential equations:

$$\begin{aligned}
&\frac{\partial}{\partial\xi}E_{x_\xi}+\frac{\partial}{\partial\eta}E_{x_\eta}+\frac{\partial}{\partial\zeta}E_{x_\zeta}=0,\\
&\frac{\partial}{\partial\xi}E_{y_\xi}+\frac{\partial}{\partial\eta}E_{y_\eta}+\frac{\partial}{\partial\zeta}E_{y_\zeta}=0,\\
&\frac{\partial}{\partial\xi}E_{z_\xi}+\frac{\partial}{\partial\eta}E_{z_\eta}+\frac{\partial}{\partial\zeta}E_{z_\zeta}=0,
\end{aligned}$$

where $E(\mathbf{r}_\xi,\mathbf{r}_\eta,\mathbf{r}_\zeta)$ is of very complicated form and to derive it one should write the elements g_{ij} in terms of the derivatives with respect to x, y, z via (8) and substitute them in the integrand of (7). Note that the elements of the covariant tensor G_{ij} (and contravariant tensor G^{ij} as well) will be involved in the coefficients of this system.

4. Non-degeneracy conditions for a cell

In the paper, we discuss the grids composed of hexahedral cells. Non-degeneracy of a grid implies that its every element is non-folded. Consider a hexahedral cell in space $\mathbb{R}^3$ of the variables x, y, z, see Fig. 2(a), which is specified via the trilinear transformation of the unit cube $I^3=\{(\xi,\eta,\zeta)\colon 0\leqslant\xi,\eta,\zeta\leqslant 1\}$ from parametric space (also called the isoparametric mapping for hexahedral finite elements)

$$\mathbf{r}=\mathbf{w}_1+\mathbf{w}_2\xi+\mathbf{w}_4\eta+\mathbf{w}_5\zeta+\mathbf{w}_3\xi\eta+\mathbf{w}_6\xi\zeta+\mathbf{w}_8\eta\zeta+\mathbf{w}_7\xi\eta\zeta, \tag{9}$$

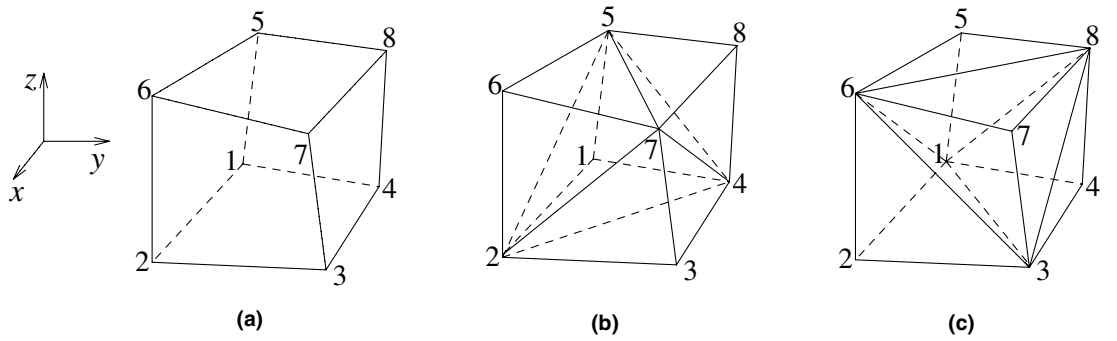

Fig. 2. Hexahedral cell (a) and two dodecahedrons of the first (b) and second (c) type with the same vertices.

where the vectors $\mathbf{w}_i$ are

$$\mathbf{w}_1 = \mathbf{r}_1, \quad \mathbf{w}_2 = \mathbf{r}_2 - \mathbf{r}_1, \quad \mathbf{w}_3 = \mathbf{r}_3 - \mathbf{r}_2 - \mathbf{r}_4 + \mathbf{r}_1, \quad \mathbf{w}_4 = \mathbf{r}_4 - \mathbf{r}_1, \quad \mathbf{w}_5 = \mathbf{r}_5 - \mathbf{r}_1,$$
$$\mathbf{w}_6 = \mathbf{r}_6 - \mathbf{r}_2 - \mathbf{r}_5 + \mathbf{r}_1, \quad \mathbf{w}_7 = \mathbf{r}_7 - \mathbf{r}_3 - \mathbf{r}_6 - \mathbf{r}_8 + \mathbf{r}_2 + \mathbf{r}_4 + \mathbf{r}_5 - \mathbf{r}_1, \quad \mathbf{w}_8 = \mathbf{r}_8 - \mathbf{r}_4 - \mathbf{r}_2 + \mathbf{r}_1$$

and $\mathbf{r}_i = (x, y, z)_i$ are the coordinates of the cell vertex.

The ruled cell in $\mathbb{R}^3$ is rather a complicated object in contrast to its analogy in $\mathbb{R}^2$, the quadrilateral cell. In the planar case to check cell non-degeneracy it is sufficient to find the value of the Jacobian J of the bilinear mapping, which transforms the unit parametric square to the quadrilateral cell, at four vertices of the cell. Saying a "non-folded cell" one implies positiveness of J at any point of the cell. In 2D, J is a linear function of coordinates within the cell. Therefore, positiveness of J at four vertices of the quadrilateral cell implies positiveness of J in the cell. In 3D, the Jacobian of the trilinear mapping (9) can be represented as the triple scalar product

$$J = \mathbf{r}_\xi \cdot (\mathbf{r}_\eta \times \mathbf{r}_\zeta),$$

where the derivatives are

$$\mathbf{r}_\xi = \mathbf{w}_2 + \mathbf{w}_3\eta + \mathbf{w}_6\zeta + \mathbf{w}_7\eta\zeta, \quad \mathbf{r}_\eta = \mathbf{w}_4 + \mathbf{w}_3\xi + \mathbf{w}_8\zeta + \mathbf{w}_7\xi\zeta, \quad \mathbf{r}_\zeta = \mathbf{w}_5 + \mathbf{w}_6\xi + \mathbf{w}_8\eta + \mathbf{w}_7\xi\eta.$$

The Jacobian is a polynomial of fourth degree depending on three variables ξ, η, ζ (maximum second degree of each) [28]. By present there is unknown a condition, being simultaneously a necessary and sufficient one, using which one may definitely say whether the ruled cell is inverted or not. One of the first investigations of this matter was executed in [38]. The most detail analysis was employed in [28,29] where it was suggested a number of necessary and sufficient non-degeneracy conditions and a numerical procedure for checking a cell if the former fails to give a definite answer. In [39], it was considered a numerical algorithm for checking invertibility for hexahedral finite elements when the isoparametric mapping is decomposed into a linear and nonlinear part.

Instead of the ruled cell, consider two dodecahedrons of the first and second type depicted in Fig. 2(b) and (c) with the same vertices. Each dodecahedron consists of the five tetrahedra: four corner ones and one internal. The trilinear mapping (9) is replaced by a set of linear transformations of the basic tetrahedra in space ξ, η, ζ to corresponding tetrahedra composing two dodecahedrons in space x, y, z. The unit cube in Fig. 3(a) is partitioned into 5 basic tetrahedra by two ways. The basic tetrahedra are the 8 corner ones (see, e.g. tetrahedron T_{1245} in Fig. 3(b)) and 2 internal ones (see, e.g. the tetrahedron T_{2457} in Fig. 3(c)). When constructing the discrete mapping $\mathbf{x}(\boldsymbol{\xi})$ we will ensure non-degeneracy of the 10 tetrahedrons composing the first and second dodecahedrons for each hexahedral cell. Thus, the non-degeneracy condition for the grid composed of dodecahedral cells of the first or second kind may be written in the form of inequalities, which will be applied in our method,

$$[V_m]_n > 0, \qquad m = 1, 2, \ldots, 10, \quad n = 1, 2, \ldots, N_c,$$

where V_m is the algebraic volume of the mth tetrahedron in the nth cell ($m = 1, 2, \ldots, 8$ corresponds to the corner tetrahedra and $m = 9$, 10 to internal), N_c is the number of the ruled cells. This condition may be rewritten in terms of J_m for the linear transformation of the basic tetrahedron since $J_m = 6V_m$. Note that at the 8 corner points (cell vertices) J_m is equal to J for (9) at these points.

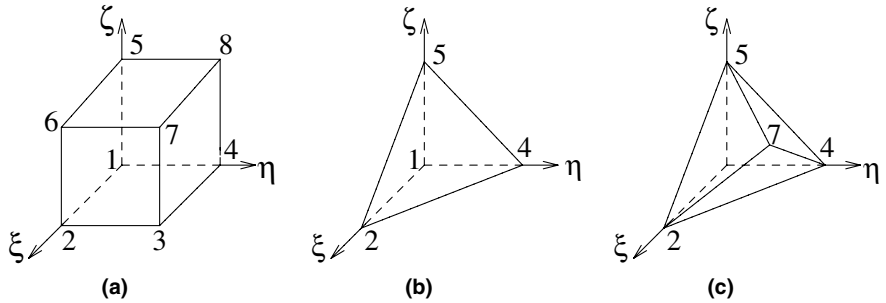

Fig. 3. In parametric space, unit cube (a) is partitioned into five basic tetrahedrons: four corner ones, like T_{1245} (b), and one internal T_{2457} (c). It is used two such partitions, see Fig. 2(b) and (c).

The non-degeneracy condition based on positiveness of the algebraic volume of only the 8 corner tetrahedrons does not prevent of folding both the hexahedral and dodecahedral cell. In [10], it was considered a counter-example of the cubic cell deformation. If to rotate the upper cube face about its center through 180°, we get a cell depicted in Fig. 4. The cell is inverted, meanwhile all the 8 corner tetrahedra have a positive algebraic volume. Thus, this condition does not prevent the cell of twisting. On the other hand the use of the 10 tetrahedrons restricts the angle of rotation by 90°. At 90°, the both internal tetrahedrons degenerate because in each one all the four vertices lie in one plane. Thus, the latter is a more reliable condition.

Next example demonstrates a difference between the sets of non-folded hexahedral and dodecahedral cells. In Table 1, the node coordinates of a hexahedron are given. This cell depicted in Fig. 5(a) and (b) is non-folded. Meanwhile the first dodecahedron has self-intersecting faces, because the internal tetrahedron T_{2457}

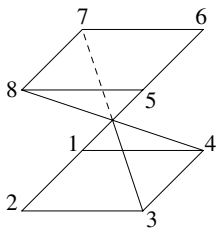

Fig. 4. Inverted cell with positive algebraic volume of 8 corner tetrahedra.

Table 1
Node coordinates

	1	2	3	4	5	6	7	8
x	0.000	0.141	0.106	−0.037	0.293	0.446	0.072	−0.073
y	0.000	−0.063	−0.144	−0.081	−0.208	−0.263	−0.225	−0.160
z	0.000	0.000	0.252	0.252	0.038	0.038	0.288	0.288

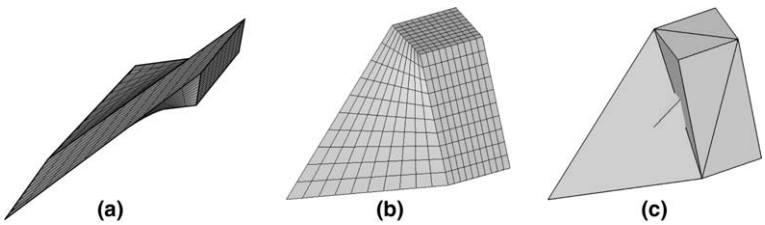

Fig. 5. Non-degenerate ruled cell, two views (a) and (b), and corresponding degenerate dodecahedron (c). In it, the tetrahedron T_{2457} is inverted.

is inverted (Jacobian $J_{T_{2457}} = -0.00155$), see Fig. 5(c). Note that the necessary condition for a ruled cell to be non-folded includes the following inequality, which was reported to the author by Ushakova:

$$V_9 + V_{10} > -\sum_{m=1}^{8} V_m.$$

It may be readily derived from the formula for the hexahedron volume V_h [28]

$$V_h = \frac{1}{2}\sum_{m=1}^{10} V_m.$$

This condition allows for a non-folded ruled cell to have at least one inverted internal tetrahedron in the corresponding dodecahedrons.

To gain a certain insight on the width (or conversely narrowness) of the non-degeneracy condition based on positiveness of the tetrahedra volume, we executed numerical experiments following mainly [28,29]. The hexahedron vertices are randomly generated in the interval $(0,1)$ in each space direction. The sampling consists of 10^7 hexahedrons. In the first experiment, at first, the sign of the algebraic volume for the 8 corner tetrahedra is checked. It is a necessary condition, that is why the cells not satisfying it are rejected. We call it C0 and the remained number of cells is given in the second column of Table 2. Below, the similar data of [28,29] is presented. The condition C0 was also applied in a numerical experiment in [38]. Afterward, we check J of the trilinear mapping in the midpoint of each cell edge, in the midpoint of each cell face, and in the midpoint of the cell. It is also a necessary condition and we call it NC1. Further J is checked on the cell edges. Since on the edge, J is a quadratic function of one parameter ξ, η, or ζ, then knowing its value at the midpoint and end-points one easily determines whether J takes a negative value within the edge. We will describe this check. Let the value of $J(\xi)$ be given at the points $\xi = 0, \frac{1}{2}, 1$ denoted by J_0, $J_{1/2}$, J_1, respectively. If at least one of these values is negative, then the cell is rejected. For the quadratic function

$$J = \alpha\xi^2 + \beta\xi + \gamma,$$

the coefficients are

$$\alpha = 2(J_0 + J_1) - 4J_{1/2}, \quad \beta = 4J_{1/2} - J_1 - 3J_0, \quad \gamma = J_0.$$

We perform the following check:

(1) if $\alpha < 0$, then $J > 0$ within the segment $\xi \in [0,1]$;
(2) if $\alpha > 0$, then the minimal value is determined via $J_\xi = 2\alpha\xi + \beta = 0$ and the minima point is $\xi_{\min} = -\beta/2\alpha$;
(3) if $\xi_{\min} \in [0,1]$, then $J_{\min} = -0.25\beta^2/\alpha + \gamma$ and the sign of $J_{\min}$ is checked;
(4) if $\xi_{\min} \notin [0,1]$, then $J > 0$ within the segment $\xi \in [0,1]$.

This necessary condition is called NC2. NC3 is the check of J on the segments joining the midpoints of the opposite edges of each face (12 segments) and on the segments joining the midpoints of the faces (3 segments). This check is executed analogously to NC2. The next condition NC4 is the check of J on the segments joining the points of the opposite faces when in parametric space each cube face is partitioned into 10×10 squares and it is performed similarly to NC2. In total it consists of $121 \times 3 = 363$ checks except for 27 already applied in

Table 2
Non-degeneracy conditions for a hexahedron

	C0	NC1	NC2	NC3	NC4	NC5
1st experiment	36,230	14,066	11,675	11,546	11,487	11,484
data of [28,29]	36,251	14,004	11,660	11,533		11,481[a]
2nd experiment	9915	7405	6881	6874	6870	6868

In the 1st experiment, C0 implies the necessary condition $V_1, \ldots, V_8 > 0$ and in 2nd the condition $V_1, \ldots, V_{10} > 0$.
[a] In [29], a computational procedure of seeking a minimum of J is employed immediately after NC3.

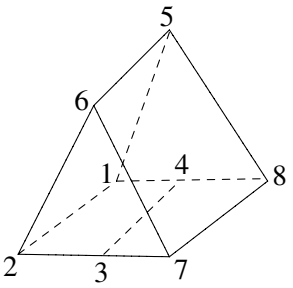

Fig. 6. Prismatic ruled cell, a hexahedron with two adjacent faces 1234 and 4378 lying in one plane.

NC2 and NC3. Generally, NC4 includes all preceding conditions, but successive implementation of the above checks reduces the number of algebraic operations by factor of tens. For reliability, the same check is executed when the cube face is partitioned into 100×100 squares and it is called NC5. After it only 3 more cells are rejected. One observes that our data is in a good compliance with that of [28,29]. In the second experiment, first all the 10 tetrahedra are checked and we call this condition C0. Further the same necessary conditions are applied as in the first experiment.

Though the number of cells in the last column of Table 2 is not equal to the one where $J > 0$, nevertheless we use it as if it is so. The experiments show that among the cells satisfying the condition $V_1, \ldots, V_8 > 0$ only 31.7% are non-folded and it was reported in [29]. The check of the 10 tetrahedra increases their share up to 69.1%. Thus, the latter is more robust. On the other hand it narrows the feasible set of non-folded cells by 40.2%.

Since the necessary conditions of the first experiment are rather close to the sufficient ones, they can be employed when testing the non-degeneracy of a 3D grid. Probably, the condition NC5, requiring much more time of execution, may be omitted. On the other hand, the initial use of the sufficient conditions of [28] reduces significantly the time of the check.

In practical implementation on the domain boundary, there may be cells in the form of the ruled triangular prism (see, e.g. [29] and Fig. 6), a hexahedron with two adjacent faces 1234 and 4378 lying in one plane. For instance, it occurs when the edge 34 lies on the bounding edge and, therefore, the faces 1234 and 4378 lie on the boundary surfaces of different families. On the edge 34, we have $J = 0$. Then, each of two corresponding dodecahedrons has one degenerated corner tetrahedron, T_{2347} and T_{1348}, because their vertices lie in one plane. Nevertheless, such cells are admissible for modeling a physical phenomena. The non-degeneracy criteria for the prismatic finite elements are considered in [40,29]. When generating a mesh, such cells must be treated in a special manner. The functional should not be discretized on intentionally degenerated tetrahedra.

5. Discretization of functional

Noting that the Jacobian of the mapping $\mathbf{x}(\boldsymbol{\xi})$ is $\sqrt{\det g} = \mathbf{r}_\xi \cdot (\mathbf{r}_\eta \times \mathbf{r}_\zeta)$ the functional (7) can be written in the form[1]

$$\mathscr{D} = \frac{1}{3^{3/2}} \int_0^1 \frac{(G^{11}g_{11} + G^{22}g_{22} + G^{33}g_{33} + 2G^{12}g_{12} + 2G^{13}g_{13} + 2G^{23}g_{23})^{3/2}\sqrt{\det G}}{\mathbf{r}_\xi \cdot (\mathbf{r}_\eta \times \mathbf{r}_\zeta)} \, \mathrm{d}\xi \, \mathrm{d}\eta \, \mathrm{d}\zeta. \tag{10}$$

Let a structured mesh of $N_i \times N_j \times N_k$ nodes be generated in the physical domain Ω. For convenience, instead of the unit cube in parametric space $\boldsymbol{\xi}$ we consider a parallelepiped with the edges $N_i - 1$, $N_j - 1$, $N_k - 1$. In every of $N_c = (N_i - 1)(N_j - 1)(N_k - 1)$ cells the functional (10) is discretized by averaging its approximation on the 10 tetrahedra forming two dodecahedrons depicted in Fig. 2(b) and (c). The resulting difference function (or discrete functional) is

[1] Recall that the mapping is assumed to be invertible and, therefore, everywhere $J > 0$.

$$\mathscr{D}^h = \frac{1}{N_c}\sum_{n=1}^{N_c}\sum_{m=1}^{10}\frac{1}{10}[E_m]_n, \tag{11}$$

where $[E_m]_n$ is the integrand in (10) computed for the mth tetrahedron in the nth cell. In Section 8, we will demonstrate that the difference function $\mathscr{D}^h$ possesses an infinite barrier on the boundary of the set of non-folded grids that prevents cells from degeneration.

If the set of non-folded grids composed of the hexahedral cells is not empty the system of the algebraic equations written for the internal nodes

$$R_x = \frac{\partial \mathscr{D}^h}{\partial x_n} = 0, \quad R_y = \frac{\partial \mathscr{D}^h}{\partial y_n} = 0, \quad R_z = \frac{\partial \mathscr{D}^h}{\partial z_n} = 0 \tag{12}$$

has at least one solution being a non-folded mesh. To find this solution we apply the unconstrained minimization taking a non-folded grid as an initial guess.

6. Minimization procedure

We use the minimization procedure for the spatial case which was also applied in [10,30]. Given a non-folded mesh at the lth iteration step, the coordinates of the nth grid node at the $l+1$th step are obtained by using the quasi-Newton procedure in the sense that in the Hessian only the diagonal elements are retained:

$$\begin{aligned}
&\tau R_x + \frac{\partial R_x}{\partial x_n}\left(x_n^{l+1} - x_n^l\right) + \frac{\partial R_x}{\partial y_n}\left(y_n^{l+1} - y_n^l\right) + \frac{\partial R_x}{\partial z_n}\left(z_n^{l+1} - z_n^l\right) = 0,\\
&\tau R_y + \frac{\partial R_y}{\partial x_n}\left(x_n^{l+1} - x_n^l\right) + \frac{\partial R_y}{\partial y_n}\left(y_n^{l+1} - y_n^l\right) + \frac{\partial R_y}{\partial z_n}\left(z_n^{l+1} - z_n^l\right) = 0,\\
&\tau R_z + \frac{\partial R_z}{\partial x_n}\left(x_n^{l+1} - x_n^l\right) + \frac{\partial R_z}{\partial y_n}\left(y_n^{l+1} - y_n^l\right) + \frac{\partial R_z}{\partial z_n}\left(z_n^{l+1} - z_n^l\right) = 0,
\end{aligned} \tag{13}$$

where τ ($\tau < 1$) is the iteration parameter. The iterations are employed until the condition

$$\max_n \left|\mathbf{r}_n^{l+1} - \mathbf{r}_n^l\right| < \varepsilon$$

is satisfied. Here $\varepsilon > 0$ is sufficiently small. To implement the minimization procedure (13) one should compute the first and second derivatives of the difference function $\mathscr{D}^h$. We will derive these formulae in the following section.

7. Computational formulae

Write the integrand in (10) in the form $F = U/V$, where

$$\begin{aligned}
&U = \gamma\left(G^{ij}g_{ji}\right)^{3/2} = \gamma\left(G^{11}g_{11} + G^{22}g_{22} + G^{33}g_{33} + 2G^{12}g_{12} + 2G^{13}g_{13} + 2G^{23}g_{23}\right)^{3/2},\\
&V = \mathbf{r}_\xi \cdot (\mathbf{r}_\eta \times \mathbf{r}_\zeta), \quad \gamma = 3^{-3/2}\sqrt{\det G}.
\end{aligned}$$

To obtain the derivatives with respect to x, y, z we use the chain rule:

$$\begin{aligned}
&F_x = \frac{U_x - FV_x}{V}, \quad F_y = \frac{U_y - FV_y}{V}, \quad F_z = \frac{U_z - FV_z}{V},\\
&F_{xx} = \frac{U_{xx} - 2F_xV_x - FV_{xx}}{V}, \quad F_{yy} = \frac{U_{yy} - 2F_yV_y - FV_{yy}}{V}, \quad F_{zz} = \frac{U_{zz} - 2F_zV_z - FV_{zz}}{V},\\
&F_{xy} = F_{yx} = \frac{U_{xy} - F_xV_y - F_yV_x - FV_{xy}}{V}, \quad F_{xz} = F_{zx} = \frac{U_{xz} - F_xV_z - F_zV_x - FV_{xz}}{V},\\
&F_{yz} = F_{zy} = \frac{U_{yz} - F_yV_z - F_zV_y - FV_{yz}}{V}.
\end{aligned} \tag{14}$$

Differentiating the numerator U yields:

$$\begin{aligned} U_x &= \frac{3}{2}\gamma\left(G^{ij}g_{ji}\right)^{1/2} G^{kl}\frac{\partial g_{lk}}{\partial x} \\ &= \frac{3}{2}\gamma\left(G^{11}g_{11}+G^{22}g_{22}+G^{33}g_{33}+2G^{12}g_{12}+2G^{13}g_{13}+2G^{23}g_{23}\right)^{1/2} \\ &\quad\times\left(G^{11}\frac{\partial g_{11}}{\partial x}+G^{22}\frac{\partial g_{22}}{\partial x}+G^{33}\frac{\partial g_{33}}{\partial x}+2G^{12}\frac{\partial g_{12}}{\partial x}+2G^{13}\frac{\partial g_{13}}{\partial x}+2G^{23}\frac{\partial g_{23}}{\partial x}\right), \\ U_{xx} &= \frac{3}{2}\gamma(G^{ij}g_{ji})^{-1/2}\left[\frac{1}{2}\left(G^{kl}\frac{\partial g_{lk}}{\partial x}\right)^2+G^{ij}g_{ji}G^{kl}\frac{\partial^2 g_{lk}}{\partial x^2}\right]. \end{aligned} \tag{15}$$

By analogy we derive the expressions for U_y, U_{yy}, U_z, U_{zz}. The resulting formulae can be derived if in (15) the variable x is replaced by y or z. The mixed derivative is

$$U_{xy} = \frac{3}{2}\gamma(G^{ij}g_{ji})^{-1/2}\left[\frac{1}{2}G^{ij}\frac{\partial g_{ji}}{\partial x}G^{kl}\frac{\partial g_{lk}}{\partial y}+G^{ij}g_{ji}G^{kl}\frac{\partial^2 g_{lk}}{\partial x\partial y}\right] \tag{16}$$

and similarly we derive U_{xz} and U_{yz}.

Consider the linear mapping $\mathbf{x}(\boldsymbol{\xi})$ which transforms the basic tetrahedron T_{1245} (see Fig. 3(b)) to the corner tetrahedron T_{1245} of the dodecahedral cell (see Fig. 2(b)). The derivatives of the vector-valued function $\mathbf{r}(\xi,\eta,\zeta)$ are approximated as follows:

$$\mathbf{r}_\xi = \mathbf{r}_2-\mathbf{r}_1, \quad \mathbf{r}_\eta = \mathbf{r}_4-\mathbf{r}_1, \quad \mathbf{r}_\zeta = \mathbf{r}_5-\mathbf{r}_1. \tag{17}$$

Recalling (8), we obtain the expressions for the metric coefficients g_{ij}:

$$\begin{aligned} &g_{11} = (\mathbf{r}_2-\mathbf{r}_1)^2, \quad g_{12} = (\mathbf{r}_2-\mathbf{r}_1)\cdot(\mathbf{r}_4-\mathbf{r}_1), \quad g_{13} = (\mathbf{r}_2-\mathbf{r}_1)\cdot(\mathbf{r}_5-\mathbf{r}_1), \\ &g_{22} = (\mathbf{r}_4-\mathbf{r}_1)^2, \quad g_{23} = (\mathbf{r}_4-\mathbf{r}_1)\cdot(\mathbf{r}_5-\mathbf{r}_1), \quad g_{33} = (\mathbf{r}_5-\mathbf{r}_1)^2. \end{aligned}$$

When computing the derivatives of U, in (15) and (16) we replace x, y, z by x_i, y_i, z_i, where i is the vertex number.

We have for vertex 1

$$\begin{aligned} &\frac{\partial g_{11}}{\partial x_1} = 2(x_1-x_2), \quad \frac{\partial^2 g_{11}}{\partial x_1^2} = 2, \quad \frac{\partial g_{12}}{\partial x_1} = 2x_1-x_2-x_4, \quad \frac{\partial^2 g_{12}}{\partial x_1^2} = 2, \\ &\frac{\partial g_{13}}{\partial x_1} = 2x_1-x_2-x_5, \quad \frac{\partial^2 g_{13}}{\partial x_1^2} = 2, \quad \frac{\partial g_{22}}{\partial x_1} = 2(x_1-x_4), \quad \frac{\partial^2 g_{22}}{\partial x_1^2} = 2, \\ &\frac{\partial g_{23}}{\partial x_1} = 2x_1-x_4-x_5, \quad \frac{\partial^2 g_{23}}{\partial x_1^2} = 2, \quad \frac{\partial g_{33}}{\partial x_1} = 2(x_1-x_5), \quad \frac{\partial^2 g_{33}}{\partial x_1^2} = 2. \end{aligned} \tag{18}$$

The derivatives with respect to y_1 and z_1 are obtained if in (18) the variables x_i are replaced by y_i, z_i. All mixed derivatives of g_{ij} with respect to x_1 and y_1, x_1 and z_1, y_1 and z_1 are equal to 0.

We have for vertex 2

$$\begin{aligned} &\frac{\partial g_{11}}{\partial x_2} = 2(x_2-x_1), \quad \frac{\partial^2 g_{11}}{\partial x_2^2} = 2, \quad \frac{\partial g_{12}}{\partial x_2} = x_4-x_1, \quad \frac{\partial^2 g_{12}}{\partial x_2^2} = 0, \quad \frac{\partial g_{13}}{\partial x_2} = x_5-x_1, \\ &\frac{\partial^2 g_{13}}{\partial x_2^2} = 0, \quad \frac{\partial g_{22}}{\partial x_2} = \frac{\partial^2 g_{22}}{\partial x_2^2} = 0, \quad \frac{\partial g_{23}}{\partial x_2} = \frac{\partial^2 g_{23}}{\partial x_2^2} = 0, \quad \frac{\partial g_{33}}{\partial x_2} = \frac{\partial^2 g_{33}}{\partial x_2^2} = 0. \end{aligned}$$

We have for vertex 4

$$\begin{aligned} &\frac{\partial g_{11}}{\partial x_4} = \frac{\partial^2 g_{11}}{\partial x_4^2} = 0, \quad \frac{\partial g_{12}}{\partial x_4} = x_2-x_1, \quad \frac{\partial^2 g_{12}}{\partial x_4^2} = 0, \quad \frac{\partial g_{13}}{\partial x_4} = \frac{\partial^2 g_{13}}{\partial x_4^2} = 0, \quad \frac{\partial g_{22}}{\partial x_4} = 2(x_4-x_1), \\ &\frac{\partial^2 g_{22}}{\partial x_4^2} = 2, \quad \frac{\partial g_{23}}{\partial x_4} = x_5-x_1, \quad \frac{\partial^2 g_{23}}{\partial x_4^2} = 0, \quad \frac{\partial g_{33}}{\partial x_4} = \frac{\partial^2 g_{33}}{\partial x_4^2} = 0. \end{aligned}$$

We have for vertex 5

$$\frac{\partial g_{11}}{\partial x_5}=\frac{\partial^2 g_{11}}{\partial x_5^2}=0,\quad \frac{\partial g_{12}}{\partial x_5}=\frac{\partial^2 g_{12}}{\partial x_5^2}=0,\quad \frac{\partial g_{13}}{\partial x_5}=x_2-x_1,\quad \frac{\partial^2 g_{13}}{\partial x_5^2}=0,\quad \frac{\partial g_{22}}{\partial x_5}=\frac{\partial^2 g_{22}}{\partial x_5^2}=0,$$
$$\frac{\partial g_{23}}{\partial x_5}=x_4-x_1,\quad \frac{\partial^2 g_{23}}{\partial x_5^2}=0,\quad \frac{\partial g_{33}}{\partial x_5}=2(x_5-x_1),\quad \frac{\partial^2 g_{33}}{\partial x_5^2}=2.$$

When differentiating the denominator V, we apply the differentiation rule for a determinant.

We have for vertex 1

$$\frac{\partial V}{\partial x_1}=\frac{\partial[\mathbf{r}_\xi\cdot(\mathbf{r}_\eta\times\mathbf{r}_\zeta)]}{\partial x_1}=\frac{\partial}{\partial x_1}\begin{vmatrix}x_2-x_1 & y_2-y_1 & z_2-z_1\\ x_4-x_1 & y_4-y_1 & z_4-z_1\\ x_5-x_1 & y_5-y_1 & z_5-z_1\end{vmatrix}=\begin{vmatrix}-1 & y_2-y_1 & z_2-z_1\\ -1 & y_4-y_1 & z_4-z_1\\ -1 & y_5-y_1 & z_5-z_1\end{vmatrix}$$
$$=y_2(z_5-z_4)+y_4(z_2-z_5)+y_5(z_4-z_2),$$

and similarly

$$\frac{\partial V}{\partial y_1}=z_2(x_5-x_4)+z_4(x_2-x_5)+z_5(x_4-x_2),\quad \frac{\partial V}{\partial z_1}=x_2(y_5-y_4)+x_4(y_2-y_5)+x_5(y_4-y_2).$$

One readily observes that all the second and mixed derivatives of V are equal to zero.

We have for vertex 2

$$\frac{\partial V}{\partial x_2}=(y_4-y_1)(z_5-z_1)-(y_5-y_1)(z_4-z_1),\quad \frac{\partial V}{\partial y_2}=(z_4-z_1)(x_5-x_1)-(z_5-z_1)(x_4-x_1),$$
$$\frac{\partial V}{\partial z_2}=(x_4-x_1)(y_5-y_1)-(x_5-x_1)(y_4-y_1).$$

We have for vertex 4

$$\frac{\partial V}{\partial x_4}=(y_5-y_1)(z_2-z_1)-(y_2-y_1)(z_5-z_1),\quad \frac{\partial V}{\partial y_4}=(z_5-z_1)(x_2-x_1)-(z_2-z_1)(x_5-x_1),$$
$$\frac{\partial V}{\partial z_4}=(x_5-x_1)(y_2-y_1)-(x_2-x_1)(y_5-y_1).$$

We have for vertex 5

$$\frac{\partial V}{\partial x_5}=(y_2-y_1)(z_4-z_1)-(y_4-y_1)(z_2-z_1),\quad \frac{\partial V}{\partial y_5}=(z_2-z_1)(x_4-x_1)-(z_4-z_1)(x_2-x_1),$$
$$\frac{\partial V}{\partial z_5}=(x_2-x_1)(y_4-y_1)-(x_4-x_1)(y_2-y_1).$$

The integrand in (10) is invariant to the coordinate system $\boldsymbol{\xi}$ rotation, therefore the above formulae may be applied to the remaining seven corner tetrahedra after the proper substitution of vertex number.

Further we derive the formulae to compute the metric coefficients g_{ij} and their derivatives for the basic tetrahedron T_{2457}, see Fig. 3(c). To approximate the derivatives the formula of averaging over the volume is applied. For instance, the derivative of a function f with respect to ξ is

$$f_\xi=\frac{1}{V_T}\int\int_{S_T} f\,\mathrm{d}\eta\,\mathrm{d}\zeta.$$

Integration is performed over the bounding surface S_T of the tetrahedron T_{2457} and V_T is its volume. The function f and its derivative f_ξ is assumed to be continuous inside the volume V_T. The derivative f_ξ in the left-hand of the relation is taken at a point $P\in V_T$.

The surface integral is partitioned into four parts (number of tetrahedron facets) and the value of f on each facet is assumed constant and equal to the averaged one over the values at three vertices. Therefore, one derives

$$f_\xi = \frac{f_2+f_4+f_5}{3V_T}\int\int_{S_{245}} \mathrm{d}\eta\,\mathrm{d}\zeta + \frac{f_2+f_4+f_7}{3V_T}\int\int_{S_{247}} \mathrm{d}\eta\,\mathrm{d}\zeta + \frac{f_2+f_5+f_7}{3V_T}\int\int_{S_{257}} \mathrm{d}\eta\,\mathrm{d}\zeta + \frac{f_4+f_5+f_7}{3V_T}\int\int_{S_{457}} \mathrm{d}\eta\,\mathrm{d}\zeta.$$

Since the area of the projection of each facet to the plane η–ζ is equal to 0.5 and the tetrahedron volume is equal to 1/3, then, taking into account the sign of the facet area (defined by the facet inclination), we obtain

$$f_\xi = \frac{1}{2}(f_7 + f_2 - f_5 - f_4).$$

Similarly one derives an approximation for f_η, f_ζ. Therefore, the derivatives of $\mathbf{r}(\xi,\eta,\zeta)$ are approximated as follows:

$$\mathbf{r}_\xi = \frac{1}{2}(\mathbf{r}_7 + \mathbf{r}_2 - \mathbf{r}_5 - \mathbf{r}_4), \quad \mathbf{r}_\eta = \frac{1}{2}(\mathbf{r}_7 + \mathbf{r}_4 - \mathbf{r}_5 - \mathbf{r}_2), \quad \mathbf{r}_\zeta = \frac{1}{2}(\mathbf{r}_7 + \mathbf{r}_5 - \mathbf{r}_2 - \mathbf{r}_4). \tag{19}$$

Recalling (8), we obtain the expressions for the metric coefficients g_{ij}:

$$g_{11} = \frac{1}{4}(\mathbf{r}_7 + \mathbf{r}_2 - \mathbf{r}_5 - \mathbf{r}_4)^2, \quad g_{12} = \frac{1}{4}(\mathbf{r}_7 + \mathbf{r}_2 - \mathbf{r}_5 - \mathbf{r}_4)\cdot(\mathbf{r}_7 + \mathbf{r}_4 - \mathbf{r}_5 - \mathbf{r}_2),$$
$$g_{22} = \frac{1}{4}(\mathbf{r}_7 + \mathbf{r}_4 - \mathbf{r}_5 - \mathbf{r}_2)^2, \quad g_{13} = \frac{1}{4}(\mathbf{r}_7 + \mathbf{r}_2 - \mathbf{r}_5 - \mathbf{r}_4)\cdot(\mathbf{r}_7 + \mathbf{r}_5 - \mathbf{r}_2 - \mathbf{r}_4),$$
$$g_{33} = \frac{1}{4}(\mathbf{r}_7 + \mathbf{r}_5 - \mathbf{r}_2 - \mathbf{r}_4)^2, \quad g_{23} = \frac{1}{4}(\mathbf{r}_7 + \mathbf{r}_4 - \mathbf{r}_5 - \mathbf{r}_2)\cdot(\mathbf{r}_7 + \mathbf{r}_5 - \mathbf{r}_2 - \mathbf{r}_4).$$

We have for vertex 2

$$\frac{\partial g_{11}}{\partial x_2} = \frac{1}{2}(x_7 + x_2 - x_5 - x_4), \quad \frac{\partial^2 g_{11}}{\partial x_2^2} = \frac{1}{2}, \quad \frac{\partial g_{12}}{\partial x_2} = \frac{1}{2}(x_4 - x_2), \quad \frac{\partial^2 g_{12}}{\partial x_2^2} = -\frac{1}{2},$$
$$\frac{\partial g_{22}}{\partial x_2} = \frac{1}{2}(x_5 + x_2 - x_7 - x_4), \quad \frac{\partial^2 g_{22}}{\partial x_2^2} = \frac{1}{2}, \quad \frac{\partial g_{13}}{\partial x_2} = \frac{1}{2}(x_5 - x_2), \quad \frac{\partial^2 g_{13}}{\partial x_2^2} = -\frac{1}{2}, \tag{20}$$
$$\frac{\partial g_{33}}{\partial x_2} = \frac{1}{2}(x_4 + x_2 - x_7 - x_5), \quad \frac{\partial^2 g_{33}}{\partial x_2^2} = \frac{1}{2}, \quad \frac{\partial g_{23}}{\partial x_2} = \frac{1}{2}(x_2 - x_7), \quad \frac{\partial^2 g_{23}}{\partial x_2^2} = \frac{1}{2}.$$

The derivatives with respect to y_2 and z_2 are obtained if in (20) the variables x_i are replaced by y_i, z_i. All mixed derivatives of g_{ij} with respect to x_2 and y_2, x_2 and z_2, y_2 and z_2 are equal to 0.

We have for vertex 4

$$\frac{\partial g_{11}}{\partial x_4} = \frac{1}{2}(x_5 + x_4 - x_7 - x_2), \quad \frac{\partial^2 g_{11}}{\partial x_4^2} = \frac{1}{2}, \quad \frac{\partial g_{12}}{\partial x_4} = \frac{1}{2}(x_2 - x_4), \quad \frac{\partial^2 g_{12}}{\partial x_4^2} = -\frac{1}{2},$$
$$\frac{\partial g_{22}}{\partial x_4} = \frac{1}{2}(x_7 + x_4 - x_5 - x_2), \quad \frac{\partial^2 g_{22}}{\partial x_4^2} = \frac{1}{2}, \quad \frac{\partial g_{13}}{\partial x_4} = \frac{1}{2}(x_4 - x_7), \quad \frac{\partial^2 g_{13}}{\partial x_4^2} = \frac{1}{2},$$
$$\frac{\partial g_{33}}{\partial x_4} = \frac{1}{2}(x_4 + x_2 - x_7 - x_5), \quad \frac{\partial^2 g_{33}}{\partial x_4^2} = \frac{1}{2}, \quad \frac{\partial g_{23}}{\partial x_4} = \frac{1}{2}(x_5 - x_4), \quad \frac{\partial^2 g_{23}}{\partial x_4^2} = -\frac{1}{2}.$$

We have for vertex 5

$$\frac{\partial g_{11}}{\partial x_5} = \frac{1}{2}(x_5 + x_4 - x_7 - x_2), \quad \frac{\partial^2 g_{11}}{\partial x_5^2} = \frac{1}{2}, \quad \frac{\partial g_{12}}{\partial x_5} = \frac{1}{2}(x_5 - x_7), \quad \frac{\partial^2 g_{12}}{\partial x_5^2} = \frac{1}{2},$$
$$\frac{\partial g_{22}}{\partial x_5} = \frac{1}{2}(x_5 + x_2 - x_7 - x_4), \quad \frac{\partial^2 g_{22}}{\partial x_5^2} = \frac{1}{2}, \quad \frac{\partial g_{13}}{\partial x_5} = \frac{1}{2}(x_2 - x_5), \quad \frac{\partial^2 g_{13}}{\partial x_5^2} = -\frac{1}{2},$$
$$\frac{\partial g_{33}}{\partial x_5} = \frac{1}{2}(x_7 + x_5 - x_2 - x_4), \quad \frac{\partial^2 g_{33}}{\partial x_5^2} = \frac{1}{2}, \quad \frac{\partial g_{23}}{\partial x_5} = \frac{1}{2}(x_4 - x_5), \quad \frac{\partial^2 g_{23}}{\partial x_5^2} = -\frac{1}{2}.$$

We have for vertex 7

$$\frac{\partial g_{11}}{\partial x_7}=\frac{1}{2}(x_7+x_2-x_5-x_4),\quad \frac{\partial^2 g_{11}}{\partial x_7^2}=\frac{1}{2},\quad \frac{\partial g_{12}}{\partial x_7}=\frac{1}{2}(x_7-x_5),\quad \frac{\partial^2 g_{12}}{\partial x_7^2}=\frac{1}{2},$$
$$\frac{\partial g_{22}}{\partial x_7}=\frac{1}{2}(x_7+x_4-x_5-x_2),\quad \frac{\partial^2 g_{22}}{\partial x_7^2}=\frac{1}{2},\quad \frac{\partial g_{13}}{\partial x_7}=\frac{1}{2}(x_7-x_4),\quad \frac{\partial^2 g_{13}}{\partial x_7^2}=\frac{1}{2},$$
$$\frac{\partial g_{33}}{\partial x_7}=\frac{1}{2}(x_7+x_5-x_2-x_4),\quad \frac{\partial^2 g_{33}}{\partial x_7^2}=\frac{1}{2},\quad \frac{\partial g_{23}}{\partial x_7}=\frac{1}{2}(x_7-x_2),\quad \frac{\partial^2 g_{23}}{\partial x_7^2}=\frac{1}{2}.$$

When differentiating the denominator V we apply the differentiation rule for a determinant.
We have for vertex 2

$$\frac{\partial V}{\partial x_2}=\frac{\partial[\mathbf{r}_\xi\cdot(\mathbf{r}_\eta\times\mathbf{r}_\zeta)]}{\partial x_2}=\frac{1}{8}\frac{\partial}{\partial x_2}\begin{vmatrix} x_7+x_2-x_5-x_4 & y_7+y_2-y_5-y_4 & z_7+z_2-z_5-z_4\\ x_7+x_4-x_5-x_2 & y_7+y_4-y_5-y_2 & z_7+z_4-z_5-z_2\\ x_7+x_5-x_2-x_4 & y_7+y_5-y_2-y_4 & z_7+z_5-z_2-z_4\end{vmatrix}$$
$$=\frac{1}{8}\begin{vmatrix} 1 & y_7+y_2-y_4-y_5 & z_7+z_2-z_4-z_5\\ -1 & y_7+y_4-y_5-y_2 & z_7+z_4-z_5-z_2\\ -1 & y_7+y_5-y_2-y_4 & z_7+z_5-z_2-z_4\end{vmatrix}=\frac{1}{2}[y_4(z_7-z_5)+y_5(z_4-z_7)+y_7(z_5-z_4)]$$

and similarly

$$\frac{\partial V}{\partial y_2}=\frac{1}{2}[z_4(x_7-x_5)+z_5(x_4-x_7)+z_7(x_5-x_4)],\quad \frac{\partial V}{\partial z_2}=\frac{1}{2}[x_4(y_7-y_5)+x_5(y_4-y_7)+x_7(y_5-y_4)].$$

It is easily seen that all the second and mixed derivatives of V are equal to zero.
We have for vertex 4

$$\frac{\partial V}{\partial x_4}=\frac{1}{2}[y_2(z_5-z_7)+y_5(z_7-z_2)+y_7(z_2-x_5)],\quad \frac{\partial V}{\partial y_4}=\frac{1}{2}[z_2(x_5-x_7)+z_5(x_7-x_2)+z_7(x_2-x_5)],$$
$$\frac{\partial V}{\partial z_4}=\frac{1}{2}[x_2(y_5-y_7)+x_5(y_7-y_2)+x_7(y_2-y_5)].$$

We have for vertex 5

$$\frac{\partial V}{\partial x_5}=\frac{1}{2}[y_2(z_7-z_4)+y_4(z_2-z_7)+y_7(z_4-z_2)],\quad \frac{\partial V}{\partial y_5}=\frac{1}{2}[z_2(x_7-x_4)+z_4(x_2-x_7)+z_7(x_4-x_2)],$$
$$\frac{\partial V}{\partial z_5}=\frac{1}{2}[x_2(y_7-y_4)+x_4(y_2-y_7)+x_7(y_4-y_2)].$$

We have for vertex 7

$$\frac{\partial V}{\partial x_7}=\frac{1}{2}[y_2(z_4-z_5)+y_4(z_5-z_2)+y_5(z_2-z_4)],\quad \frac{\partial V}{\partial y_7}=\frac{1}{2}[z_2(x_4-x_5)+z_4(x_5-x_2)+z_5(x_2-x_4)],$$
$$\frac{\partial V}{\partial z_7}=\frac{1}{2}[x_2(y_4-y_5)+x_4(y_5-y_2)+x_5(y_2-y_4)].$$

For the second basic internal tetrahedron, which is transformed to the tetrahedron T_{1368}, see Fig. 2(b), we apply the above formulae with proper substitution of the vertex number.

Given the value of F and its derivatives at the vertices of the 10 tetrahedrons, we form the elements of the system for the quasi-Newton procedure (13). Let the local vertex numbers $1,2,\ldots,8$ in the cell correspond to the global grid node numbers $n_1,n_2,\ldots,n_8$. Then the value of F and its derivatives in vertex 1 of the tetrahedron T_{1245} are added to $\mathscr{D}^h$ and elements of the system (13)

$$\mathscr{D}^h = \mathscr{D}^h + F, \quad [R_x]_{n_1} = [R_x]_{n_1} + F_x, \quad [R_y]_{n_1} = [R_y]_{n_1} + F_y, \quad [R_z]_{n_1} = [R_z]_{n_1} + F_z,$$
$$[R_{xx}]_{n_1} = [R_{xx}]_{n_1} + F_{xx}, \quad [R_{yy}]_{n_1} = [R_{yy}]_{n_1} + F_{yy}, \quad [R_{zz}]_{n_1} = [R_{zz}]_{n_1} + F_{zz},$$
$$[R_{xy}]_{n_1} = [R_{xy}]_{n_1} + F_{xy}, \quad [R_{xz}]_{n_1} = [R_{xz}]_{n_1} + F_{xz}, \quad [R_{yz}]_{n_1} = [R_{yz}]_{n_1} + F_{yz}.$$

Here it is employed a notation drawn in programming languages. It implies, for instance, that a new value of $\mathscr{D}^h$ is equal to $\mathscr{D}^h + F$. The values in vertices 2, 4, 5 of the tetrahedron are added to $\mathscr{D}^h$ and corresponding elements $[R_x]_{n_2}, \ldots, [R_x]_{n_4}, \ldots, [R_x]_{n_5}, \ldots$ Similarly we treat F and its derivatives calculated at the vertices of the 9 remaining tetrahedrons.

The method can be extended to unstructured grids in a straightforward manner. One needs only to define a correspondence between a local vertex number in a cell and a global grid node number.

8. Barrier property of $\mathscr{D}^h$

Prior to proceed to the consideration of the barrier property of the discrete functional, let us write the integrand E of (10) in the form suitable for the analysis. Due to invariance of E to the orthogonal transformations of the coordinates X, Y, Z, at any point of the parametric cube, it can be presented in a coordinate system where G is a diagonal matrix, i.e.,

$$E = \frac{(\mathrm{tr}(G^{-1}g))^{3/2}}{\sqrt{\det(G^{-1}g)}} = \frac{(\tilde{\lambda}_i g_{ii})^{3/2}}{\sqrt{\det g}\sqrt{\tilde{\lambda}_1\tilde{\lambda}_2\tilde{\lambda}_3}}, \tag{21}$$

where $\tilde{\lambda}_i$ are the eigenvalues of the matrix G^{-1}.

The function $\mathscr{D}^h$ possesses a barrier property formulated as the following theorem:

Theorem. *The function $\mathscr{D}^h$ possesses an infinite barrier on the boundary of the set of non-folded grids composed of dodecahedral cells of the first or second kind.*

Proof. Suppose some dodecahedral cell, say the first type (see Fig. 2(b)), degenerates. This is due to at least one of five tetrahedrons, composing this cell, degenerates. It may be a corner tetrahedron, say T_{1245}, or internal T_{2457}. Consider the approximation of (21) for T_{1245} and T_{2457}. Let the tetrahedron volume tend to 0, while remaining positive, i.e., the Jacobian $\sqrt{\det g} \to 0$. For $\mathscr{D}^h$ not to tend to $+\infty$, the approximation of the numerator in (21) must tend to zero as well. In other words for the tetrahedron T_{1245}

$$\tilde{\lambda}_1 g_{11} + \tilde{\lambda}_2 g_{22} + \tilde{\lambda}_3 g_{33} = \tilde{\lambda}_1(\mathbf{r}_2 - \mathbf{r}_1)^2 + \tilde{\lambda}_2(\mathbf{r}_4 - \mathbf{r}_1)^2 + \tilde{\lambda}_3(\mathbf{r}_5 - \mathbf{r}_1)^2 \to 0$$

(due to invariance of the approximating formulae to the coordinate system rotation, a similar approximation holds validity for any of the remaining 3 corner tetrahedrons) and for tetrahedron T_{2457}

$$\tilde{\lambda}_1(\mathbf{r}_7 + \mathbf{r}_2 - \mathbf{r}_5 - \mathbf{r}_4)^2 + \tilde{\lambda}_2(\mathbf{r}_7 + \mathbf{r}_4 - \mathbf{r}_5 - \mathbf{r}_2)^2 + \tilde{\lambda}_3(\mathbf{r}_7 + \mathbf{r}_5 - \mathbf{r}_2 - \mathbf{r}_4)^2 \to 0.$$

Since all $\tilde{\lambda}_i > 0$, then all the tetrahedron vertices must shrink to a point. Each of T_{1245} and T_{2457} has a common edge or face with the remaining 4 tetrahedrons. Therefore, the remaining tetrahedrons degenerate too and their volume tends to 0. Analysis, similar to above, gives that for $\mathscr{D}^h$ not to tend to $+\infty$, all the vertices of these 4 tetrahedrons must shrink to a point. Thus, all the cell vertices must shrink to a point. Looking through sequentially all the cells we obtain that all the grid nodes will shrink to a point and this is in a contradiction with boundary nodes redistribution on the domain boundary. For the second type cell (see Fig. 2c), the proof is performed in the same manner. □

Due to the infinite barrier on the boundary of the set of non-folded grids, we may specify such a minimization parameter τ in the procedure (13) that the mesh will remain non-folded.

In 3D, the barrier property of the discrete functional was applied in [10,30], while instead of the trilinear mapping of the parametric cube to the hexahedron it is applied a linear transformation of the 24 basic tetrahedra (different from considered in the present paper) to the corresponding tetrahedra in the physical domain.

9. Boundary nodes redistribution

If when modeling the main problem, the boundary of the domain Ω moves and its shape changes substantially, it is required to redistribute the mesh nodes over the boundary $\partial\Omega$. In [41], for the 2D case it was suggested such an algorithm, a constrained minimization of the functional. This algorithm allows to construct a nearly conformal mapping (conformal one with an additional parameter, so called conformal modulus) and a corresponding mesh in 2D domains [22]. Here we extend it to the 3D case.

In the suggested approach, the problem of the constrained minimization of $\mathscr{D}^h$ is solved subject to constraints defining the boundary $\partial\Omega$. The following discrete functional is to be minimized

$$\mathscr{D}_1^h = \frac{1}{N_c}\sum_{n=1}^{N_c}\sum_{m=1}^{10}\frac{1}{10}[E_m]_n + \sum_{\mathbf{r}_l\in\partial\Omega}\lambda_l Q(\mathbf{r}_l) = \mathscr{D}^h + \sum_{l\in\mathscr{L}}\lambda_l Q_l; \tag{22}$$

here the constraints $Q_l = Q(\mathbf{r}_l) = 0$ define $\partial\Omega$, λ_l are the Lagrange multipliers, and $\mathscr{L}$ is the set of the boundary nodes. Since the function $Q(\mathbf{r})$ is assumed piecewise differentiable, the difference function $\mathscr{D}_1^h$ holds the infinite barrier on the boundary of the set of non-folded grids composed of dodecahedral cells.

Now the system of algebraic equations, analogous to (12), will be supplemented with the constraints

$$R_x = \frac{\partial\mathscr{D}^h}{\partial x_n} + \lambda_n\frac{\partial Q_n}{\partial x_n} = 0, \quad R_y = \frac{\partial\mathscr{D}^h}{\partial y_n} + \lambda_n\frac{\partial Q_n}{\partial y_n} = 0, \quad R_z = \frac{\partial\mathscr{D}^h}{\partial z_n} + \lambda_n\frac{\partial Q_n}{\partial z_n} = 0, \quad Q_n = 0; \tag{23}$$

here $\lambda_n = 0$ if $n \notin \mathscr{L}$ and constraints are defined for the boundary nodes $n \in \mathscr{L}$.

Consider the method of minimizing the function (22) assuming the mesh to be non-folded at the lth step of the iterative procedure. We use the quasi-Newton procedure to find the coordinates $x_n^{l+1}, y_n^{l+1}, z_n^{l+1}$ of the nth node at the $l+1$th step:

$$\begin{aligned}
&\tau R_x + \frac{\partial R_x}{\partial x_n}\left(x_n^{l+1}-x_n^l\right) + \frac{\partial R_x}{\partial y_n}\left(y_n^{l+1}-y_n^l\right) + \frac{\partial R_x}{\partial z_n}\left(z_n^{l+1}-z_n^l\right) + \frac{\partial R_x}{\partial \lambda_n}\left(\lambda_n^{l+1}-\lambda_n^l\right) = 0,\\
&\tau R_y + \frac{\partial R_y}{\partial x_n}\left(x_n^{l+1}-x_n^l\right) + \frac{\partial R_y}{\partial y_n}\left(y_n^{l+1}-y_n^l\right) + \frac{\partial R_y}{\partial z_n}\left(z_n^{l+1}-z_n^l\right) + \frac{\partial R_y}{\partial \lambda_n}\left(\lambda_n^{l+1}-\lambda_n^l\right) = 0,\\
&\tau R_z + \frac{\partial R_z}{\partial x_n}\left(x_n^{l+1}-x_n^l\right) + \frac{\partial R_z}{\partial y_n}\left(y_n^{l+1}-y_n^l\right) + \frac{\partial R_z}{\partial z_n}\left(z_n^{l+1}-z_n^l\right) + \frac{\partial R_z}{\partial \lambda_n}\left(\lambda_n^{l+1}-\lambda_n^l\right) = 0,\\
&\tau Q_n + \frac{\partial Q_n}{\partial x_n}\left(x_n^{l+1}-x_n^l\right) + \frac{\partial Q_n}{\partial y_n}\left(y_n^{l+1}-y_n^l\right) + \frac{\partial Q_n}{\partial z_n}\left(z_n^{l+1}-z_n^l\right) = 0,
\end{aligned} \tag{24}$$

where, for instance,

$$\frac{\partial R_x}{\partial x_n} = \frac{\partial^2\mathscr{D}^h}{\partial x_n^2} + \lambda_n\frac{\partial^2 Q_n}{\partial x_n^2}, \quad \frac{\partial R_x}{\partial y_n} = \frac{\partial^2\mathscr{D}^h}{\partial x_n\partial y_n} + \lambda_n\frac{\partial^2 Q_n}{\partial x_n\partial y_n}, \quad \frac{\partial R_x}{\partial z_n} = \frac{\partial^2\mathscr{D}^h}{\partial x_n\partial z_n} + \lambda_n\frac{\partial^2 Q_n}{\partial x_n\partial z_n}, \quad \frac{\partial R_x}{\partial \lambda_n} = \frac{\partial Q_n}{\partial x_n},$$

and similarly the derivatives of R_y and R_z are defined.

Resolving the last equation of (24) about $z_n^{l+1} - z_n^l$ and substituting it in the three remaining equations, we get the system

$$\begin{pmatrix} a_{11} & a_{12} & a_{13}\\ a_{21} & a_{22} & a_{23}\\ a_{31} & a_{32} & a_{33}\end{pmatrix}\begin{pmatrix} x_n^{l+1}-x_n^l\\ y_n^{l+1}-y_n^l\\ \lambda_n^{l+1}-\lambda_n^l\end{pmatrix} = \begin{pmatrix} a_{14}\\ a_{24}\\ a_{34}\end{pmatrix}, \tag{25}$$

where

$$a_{11}=\frac{\partial R_x}{\partial x_n}-\alpha\frac{\partial R_x}{\partial z_n},\quad a_{12}=\frac{\partial R_x}{\partial y_n}-\beta\frac{\partial R_x}{\partial z_n},\quad a_{13}=\frac{\partial R_x}{\partial \lambda_n}=\frac{\partial Q_n}{\partial x_n},$$
$$a_{21}=\frac{\partial R_y}{\partial x_n}-\alpha\frac{\partial R_y}{\partial z_n},\quad a_{22}=\frac{\partial R_y}{\partial y_n}-\beta\frac{\partial R_y}{\partial z_n},\quad a_{23}=\frac{\partial R_y}{\partial \lambda_n}=\frac{\partial Q_n}{\partial y_n},$$
$$a_{31}=\frac{\partial R_z}{\partial x_n}-\alpha\frac{\partial R_z}{\partial z_n},\quad a_{32}=\frac{\partial R_z}{\partial y_n}-\beta\frac{\partial R_z}{\partial z_n},\quad a_{33}=\frac{\partial R_z}{\partial \lambda_n}=\frac{\partial Q_n}{\partial z_n},$$
$$a_{14}=\tau\left[Q_n\frac{\partial R_x}{\partial z_n}\left(\frac{\partial Q_n}{\partial z_n}\right)^{-1}-R_x\right]=-\tau R_x,\quad a_{24}=-\tau R_y,\quad a_{34}=-\tau R_z,$$
$$\alpha=\frac{\partial Q_n}{\partial x_n}\left(\frac{\partial Q_n}{\partial z_n}\right)^{-1},\quad \beta=\frac{\partial Q_n}{\partial y_n}\left(\frac{\partial Q_n}{\partial z_n}\right)^{-1}.$$

The system (25) is resolved about x_n^{l+1}, y_n^{l+1}, λ_n^{l+1}. Further, from the third equation of (24) we find z_n^{l+1}. If the constraints are resolved about z in the form $Q=z-q_1(x,y)=0$, then

$$\frac{\partial Q_n}{\partial x_n}=-\frac{\partial q_{1n}}{\partial x_n},\quad \frac{\partial Q_n}{\partial y_n}=-\frac{\partial q_{1n}}{\partial y_n},\quad \frac{\partial Q_n}{\partial z_n}=1$$

and the above formulas are simplified.

The constraints can be resolved about y in the form $Q=y-q_2(x,z)=0$, then

$$\frac{\partial Q_n}{\partial x_n}=-\frac{\partial q_{2n}}{\partial x_n},\quad \frac{\partial Q_n}{\partial y_n}=1,\quad \frac{\partial Q_n}{\partial z_n}=-\frac{\partial q_{2n}}{\partial z_n}.$$

Resolving the last equation of (24) about $y_n^{l+1}-y_n^l$ and substituting it in the three remaining equations, we get the system similar to (25) with new coefficients:

$$a_{11}=\frac{\partial R_x}{\partial x_n}-\alpha\frac{\partial R_x}{\partial y_n},\quad a_{12}=\frac{\partial R_x}{\partial z_n}-\beta\frac{\partial R_x}{\partial y_n},$$
$$a_{21}=\frac{\partial R_y}{\partial x_n}-\alpha\frac{\partial R_y}{\partial y_n},\quad a_{22}=\frac{\partial R_y}{\partial z_n}-\beta\frac{\partial R_y}{\partial y_n},$$
$$a_{31}=\frac{\partial R_z}{\partial x_n}-\alpha\frac{\partial R_z}{\partial y_n},\quad a_{32}=\frac{\partial R_z}{\partial z_n}-\beta\frac{\partial R_z}{\partial y_n},$$
$$\alpha=-\frac{\partial q_{2n}}{\partial x_n},\quad \beta=-\frac{\partial q_{2n}}{\partial z_n}.$$

Remaining coefficients do not change. The system is resolved about x_n^{l+1}, z_n^{l+1}, λ_n^{l+1}. Further, from the second equation of (24), we find y_n^{l+1}.

The constraints can be resolved about x in the form $Q=x-q_3(y,z)=0$, then

$$\frac{\partial Q_n}{\partial x_n}=1,\quad \frac{\partial Q_n}{\partial y_n}=-\frac{\partial q_{3n}}{\partial y_n},\quad \frac{\partial Q_n}{\partial z_n}=-\frac{\partial q_{3n}}{\partial z_n}.$$

Resolving the last equation of (24) about $x_n^{l+1}-x_n^l$ and substituting it in the three remaining equations, we get the system similar to (25) with new coefficients:

$$a_{11}=\frac{\partial R_x}{\partial y_n}-\alpha\frac{\partial R_x}{\partial x_n},\quad a_{12}=\frac{\partial R_x}{\partial z_n}-\beta\frac{\partial R_x}{\partial x_n},$$
$$a_{21}=\frac{\partial R_y}{\partial y_n}-\alpha\frac{\partial R_y}{\partial x_n},\quad a_{22}=\frac{\partial R_y}{\partial z_n}-\beta\frac{\partial R_y}{\partial x_n},$$
$$a_{31}=\frac{\partial R_z}{\partial y_n}-\alpha\frac{\partial R_z}{\partial x_n},\quad a_{32}=\frac{\partial R_z}{\partial z_n}-\beta\frac{\partial R_z}{\partial x_n},$$
$$\alpha=-\frac{\partial q_{3n}}{\partial y_n},\quad \beta=-\frac{\partial q_{3n}}{\partial z_n}.$$

Remaining coefficients do not change. The system is resolved about y_n^{l+1}, z_n^{l+1}, λ_n^{l+1}. Further, from the first equation of (24), we find x_n^{l+1}.

These three forms of $Q(\mathbf{r})$ can substitute for each other. On the part of $\partial\Omega$ where the tangent plane to $\partial\Omega$ is nearly parallel to the plane x–y the boundary should be defined in the form $z = q_1(x,y)$. Where it is nearly parallel to the plane x–z the boundary should be defined in the form $y = q_2(x,z)$, and where it is nearly parallel to the plane y–z the boundary should be defined in the form $x = q_3(y,z)$. If we need to move the boundary nodes along the bounding edge, being the intersection line between the different bounding surfaces, say $q_1(x,y)$ and $q_2(x,z)$, then after determining x_n^{l+1} we find y_n^{l+1} from the equation of this edge $q_1(x,y) = q_2(x,z)$.

If the boundary is defined parametrically in the form $\boldsymbol{r}(u,v)$ (u,v are parameters), then the following procedure of the unconstrained minimization can be applied. The parameters (and node coordinates as well) at the $l+1$th step are updated by using the quasi-Newton procedure:

$$\begin{aligned} &\tau R_u + R_{uu}\left(u_n^{l+1} - u_n^l\right) + R_{uv}\left(v_n^{l+1} - v_n^l\right) = 0,\\ &\tau R_v + R_{uv}\left(u_n^{l+1} - u_n^l\right) + R_{vv}\left(v_n^{l+1} - v_n^l\right) = 0, \end{aligned} \tag{26}$$

where

$$R_u = \frac{\partial R}{\partial u_n} = R_x\frac{\partial x_n}{\partial u_n} + R_y\frac{\partial y_n}{\partial u_n} + R_z\frac{\partial z_n}{\partial u_n}, \quad R_v = \frac{\partial R}{\partial v_n} = R_x\frac{\partial x_n}{\partial v_n} + R_y\frac{\partial y_n}{\partial v_n} + R_z\frac{\partial z_n}{\partial v_n},$$

$$\begin{aligned} R_{uu} = \frac{\partial^2 R}{\partial u_n^2} &= R_x\frac{\partial^2 x_n}{\partial u_n^2} + \left(R_{xx}\frac{\partial x_n}{\partial u_n} + R_{xy}\frac{\partial y_n}{\partial u_n} + R_{xz}\frac{\partial z_n}{\partial u_n}\right)\frac{\partial x_n}{\partial u_n} + R_y\frac{\partial^2 y_n}{\partial u_n^2}\\ &+ \left(R_{xy}\frac{\partial x_n}{\partial u_n} + R_{yy}\frac{\partial y_n}{\partial u_n} + R_{yz}\frac{\partial z_n}{\partial u_n}\right)\frac{\partial y_n}{\partial u_n} + R_z\frac{\partial^2 z_n}{\partial u_n^2} + \left(R_{xz}\frac{\partial x_n}{\partial u_n} + R_{yz}\frac{\partial y_n}{\partial u_n} + R_{zz}\frac{\partial z_n}{\partial u_n}\right)\frac{\partial z_n}{\partial u_n}, \end{aligned}$$

$$\begin{aligned} R_{vv} = \frac{\partial^2 R}{\partial v_n^2} &= R_x\frac{\partial^2 x_n}{\partial v_n^2} + \left(R_{xx}\frac{\partial x_n}{\partial v_n} + R_{xy}\frac{\partial y_n}{\partial v_n} + R_{xz}\frac{\partial z_n}{\partial v_n}\right)\frac{\partial x_n}{\partial v_n} + R_y\frac{\partial^2 y_n}{\partial v_n^2}\\ &+ \left(R_{xy}\frac{\partial x_n}{\partial v_n} + R_{yy}\frac{\partial y_n}{\partial v_n} + R_{yz}\frac{\partial z_n}{\partial v_n}\right)\frac{\partial y_n}{\partial v_n} + R_z\frac{\partial^2 z_n}{\partial v_n^2} + \left(R_{xz}\frac{\partial x_n}{\partial v_n} + R_{yz}\frac{\partial y_n}{\partial v_n} + R_{zz}\frac{\partial z_n}{\partial v_n}\right)\frac{\partial z_n}{\partial v_n}, \end{aligned}$$

$$\begin{aligned} R_{uv} = \frac{\partial^2 R}{\partial u_n \partial v_n} &= R_x\frac{\partial^2 x_n}{\partial u_n \partial v_n} + \left(R_{xx}\frac{\partial x_n}{\partial v_n} + R_{xy}\frac{\partial y_n}{\partial v_n} + R_{xz}\frac{\partial z_n}{\partial v_n}\right)\frac{\partial x_n}{\partial u_n} + R_y\frac{\partial^2 y_n}{\partial u_n \partial v_n}\\ &+ \left(R_{xy}\frac{\partial x_n}{\partial v_n} + R_{yy}\frac{\partial y_n}{\partial v_n} + R_{yz}\frac{\partial z_n}{\partial v_n}\right)\frac{\partial y_n}{\partial u_n} + R_z\frac{\partial^2 z_n}{\partial u_n \partial v_n} + \left(R_{xz}\frac{\partial x_n}{\partial v_n} + R_{yz}\frac{\partial y_n}{\partial v_n} + R_{zz}\frac{\partial z_n}{\partial v_n}\right)\frac{\partial z_n}{\partial u_n}. \end{aligned}$$

Resolving the system (26) we have:

$$\begin{aligned} u_n^{l+1} &= u_n^l - \tau(R_u R_{vv} - R_v R_{uv})\left(R_{uu}R_{vv} - R_{uv}^2\right)^{-1},\\ v_n^{l+1} &= v_n^l - \tau(R_v R_{uu} - R_u R_{uv})\left(R_{uu}R_{vv} - R_{uv}^2\right)^{-1}. \end{aligned}$$

On the bounding edge, where only one parameter is variable, say u, its value at the $l+1$th step is calculated via the Newton procedure

$$\tau R_u + R_{uu}\left(u_n^{l+1} - u_n^l\right) = 0.$$

From it, one obtains

$$u_n^{l+1} = u_n^l - \tau R_u / R_{uu}.$$

10. Mesh condensing and orthogonalization near the boundary

Sometimes it is required that coordinate lines of the mesh approach orthogonally the boundary $\partial\Omega$. It may be done by specifying the metric G. The task in hand is the following. Moving away from $\partial\Omega$ to the interior of Ω, several cell layers (called boundary cell layers) should be constructed with given node coordinates subject to the orthogonality condition and, if necessary, grid surfaces condensing towards $\partial\Omega$. Generally speaking, the

orthogonality condition may be specified by the user himself. These boundary cell layers define the metric g and, therefore, metric $G = g$. Afterward, it follows the transition cell layers where the metric G transforms from given in the boundary cell layers to the Euclidian metric in the last cell layer that corresponds to obtaining a quasi-uniform mesh in the interior of Ω.

Near $\partial\Omega$, we construct the orthogonal mesh by the conventional marching algorithm. Let on the boundary $\partial\Omega$, given parametrically $\mathbf{r} = \mathbf{r}(\xi, \eta)$, the mesh of quadrilateral cells be given. For definiteness, let this boundary be the coordinate surface $k = 1$. To build the coordinate surface $k = 2$ one needs to know the inward normal vector at the node $(i, j, 1)$, see Fig. 7. The inward unit normal vector is

$$\mathbf{n}_{i,j,1} = \frac{\mathbf{r}_\xi \times \mathbf{r}_\eta}{|\mathbf{r}_\xi \times \mathbf{r}_\eta|}.$$

Here $\mathbf{r}_\xi$ and $\mathbf{r}_\eta$, the tangential vectors towards the surface along the coordinate lines ξ and η, respectively, are computed via the finite-difference approximation for the derivatives

$$\mathbf{r}_\xi = 0.5(\mathbf{r}_{i+1,j,1} - \mathbf{r}_{i-1,j,1}), \quad \mathbf{r}_\eta = 0.5(\mathbf{r}_{i,j+1,1} - \mathbf{r}_{i,j-1,1}).$$

Given the distance Δl between the nodes, we find the node coordinates on the next coordinate surface $k = 2$

$$\mathbf{r}_{i,j,2} = \mathbf{r}_{i,j,1} + \mathbf{n}_{i,j,1}\Delta l. \tag{27}$$

Further, we find the metric G in the first boundary cell layer. Moving layer by layer away from $\partial\Omega$, we change the parameter Δl from initial small in the first cell layer $k = 1$ to certain given in the cell layer $k = k_0$ by a polynomial law (generally the quadric dependence is sufficient) so as to obtain grid surfaces impaction towards $\partial\Omega$.

Afterward, within several transition cell layers, say k_{trn}, the metric G should be transformed to Euclidian, because in the interior of the physical domain, far from $\partial\Omega$, generally, the quasi-uniform grid is required which is defined through the cubic cells in space X, Y, Z. To this end, the $(i + 1/2, j + 1/2, k_0 + 1/2)$th hexahedral cell from the k_0th boundary cell layer in space X, Y, Z should be transformed to a unit cube within k_{trn} cell layers. Superpose the cube vertex 1 with the cell vertex 1, see Fig. 8. The remaining 7 cell vertices come to the correspondent cube vertices using a linear interpolation within k_{trn} layers

$$\mathbf{r}_i = \mathbf{r}_i^{\text{h}} + \frac{k - k_0}{k_{\text{trn}}}(\mathbf{r}_i^{\text{c}} - \mathbf{r}_i^{\text{h}}), \quad i = 2, \ldots, 8, \; k = k_0 + 1, \ldots, k_0 + k_{\text{trn}},$$

where $\mathbf{r}_i^{\text{h}}, \mathbf{r}_i^{\text{c}}$ are the coordinates of the ith vertex of the hexahedron and cube, respectively. Due to the functional (7) is invariant, it is not necessary to rotate the cube about the ruled cell and elongate/compress its edges.

If when passing from the k_0th cell layer to the $k_0 + 1$th one, the coordinate line bends sharply, then this bend can be smoothed. In the boundary cell layers the grid line direction (i.e., components of the vector defining the line direction) should be smoothly (linearly) changed from orthogonal to $\partial\Omega$ to the given direction in

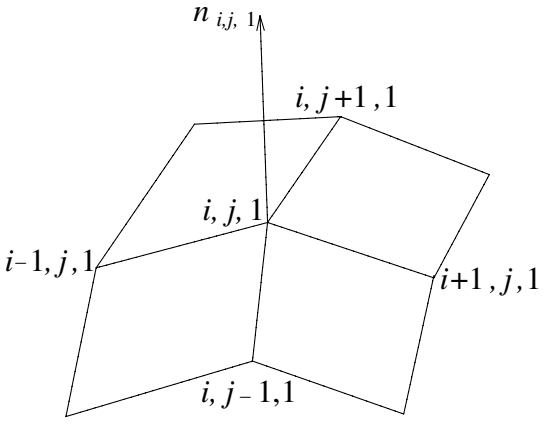

Fig. 7. Grid orthogonalization near $\partial\Omega$. $\mathbf{n}_{i,j,1}$ is the inward unit normal vector on $\partial\Omega$.

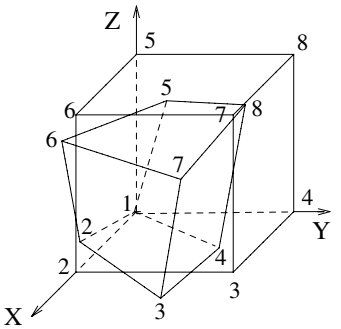

Fig. 8. Ruled cell of the last boundary layer k_0 is transformed to a unit cube within k_{trn} cell layers.

the k_0th cell layer. Sometimes this direction may be given by the correspondent cell edge in the $k_o + 1$th layer. Such a technique should be used in the vicinity of a non-smoothness of $\partial\Omega$ (sharp break, corner, etc.) where the orthogonal mesh cannot be constructed in principle.

We use the variational formulation 2, since beginning with the transition cell layer to define the metric G it is only applied the cell-to-cell transformation regardless how the cells are settled relatively each other in space X, Y, Z.

Here it may emerge a difficulty which has not been met in 2D considered in [21]. The cells of the boundary layer in space X, Y, Z defining the metric G may be inverted. In other words, the matrix G is not positive definite. This, in turn, leads to degeneration of the corresponding cells in the physical domain Ω. In Section 12, it is presented an example of constructing the orthogonal mesh when for the cells of the boundary layer one internal tetrahedra, T_{2457} or T_{1368}, degenerates. As noted in Section 4 the non-degeneracy condition, where the 10 tetrahedra are checked, narrows the feasible set of non-folded ruled cells. Then the functional (7) should be discretized only on the 8 corner tetrahedra. On the other hand this condition cannot guarantee cell non-degeneracy in much more events (see, e.g. Fig. 4). One of the ways to overcome this difficulty is to refuse of mesh orthogonality near the boundary holding only condensation. Then in space X, Y, Z we construct a parallelepipedal grid with a variable cell size in the normal direction to the boundary. Another way is to combine these two conditions, i.e., to discretize the functional on the 8 tetrahedra in the boundary cell layer and on the 10 tetrahedra in the interior of Ω. One more way is that the mesh on the bounding surface in the vicinity of a strong curvature can be refined. Then the cells will not over-twist vastly and will be non-degenerate.

11. Mesh untangling

The minimization procedure (13) for the difference function $\mathscr{D}^h$ is applied provided that the initial mesh is non-folded. In a domain of complicated geometry, construction of the initial non-folded mesh is a separate problem. In 2D, generally, it is used a penalization term for the inverted or non-convex quadrilateral cells (see, e.g. [8,30,42]). For instance in [30], when treating the functional (5) in the cells where J is negative, its value is replaced by a small positive value. Since J is in the denominator of the integrand, the discrete functional is penalized in the cell being a degenerate or non-convex quadrilateral. In 2D, this technique is successful. However, the 3D analog of the penalization algorithm of [30] did not ensure mesh untangling even if Ω is the simplest cubic domain with an initial tangled (folded) grid. In [37], it was suggested a regularization of the functional (5) so as to pass smoothly through the infinite barrier while untangling a cell. We employ a 3D analog of the regularized functional. In the denominator of (10), instead of J we use

$$J_\varepsilon = 0.5J + 0.5\sqrt{J^2 + \varepsilon^2}; \tag{28}$$

here $\varepsilon > 0$ is sufficiently small. When discretizing, as ε it may be taken

$$\varepsilon = \max(\max|V_{\text{neg}}|, \delta),$$

where V_{neg} is a negative algebraic volume of the tetrahedron and all inverted tetrahedra are examined. $\delta = 10^{-10} - 10^{-8}$ defines the lower boundary of ε to avoid emergence of very large values. In the feasible set

of non-folded grids, the regularized discrete functional is an infinite differentiable function with respect to its arguments and is close to (11). While moving away from the feasible set, it tends to $+\infty$. The untangling procedure should be applied with the Euclidian metric G. After constructing a non-folded initial mesh, one may apply the Riemannian metric G. In [43], a regularization similar to (28) is applied for the surface triangular grid construction.

12. Examples of mesh

12.1. Wavelet domain

A mesh of $21 \times 21 \times 21$ nodes is generated in the following domain: $-1 \leqslant x, y \leqslant 1$, the bottom boundary is the plane $z = -0.5$, the upper boundary is the surface

$$z(x,y) = \begin{cases} 0 & \text{if } f \leqslant 0 \quad \text{or} \quad \gamma > \pi, \\ f & \text{otherwise,} \end{cases}$$

where $f = 1 + \cos\gamma$, $\gamma = \alpha^{3/2}\sqrt{0.5x^2 + y^2}$, $\alpha = 3$.

The initial mesh is generated using a transfinite interpolation, see the mesh on the bounding surface in Fig. 9(a) and the coordinate surface $i = 11$ in the plane of symmetry $x = 0$ in Fig. 9(b). The same coordinate surface of the mesh generated by the present method with the Euclidian metric G is shown in Fig. 10 and in the next figures this surface will be shown as well. Here the functional minimum is $\mathscr{D}^h_{\min} = 2.25$. If to compute the metric g and define $G = g$, minimizing $\mathscr{D}^h$ produces the same mesh, while the absolute minimum of the discrete functional is attained, i.e., $\mathscr{D}^h_{\min} = 1$. Next calculation is executed applying grid condensing towards the upper boundary, see Fig. 11. In the canonical domain, it is given a parallelepipedal mesh with surfaces impaction towards the upper boundary by the parabolic law. Within the 10 cell layers the cell size in Z changes from 0.01 in the 1st upper layer to 1 in the 10th layer that corresponds to the cubic cell in space X, Y, Z, i.e., the metric G is Euclidian in the interior. The functional minimum is $\mathscr{D}^h_{\min} = 2.83$. Further, the constrained minimization (24) is used to move the nodes on the bounding surfaces and edges, see Fig. 12, with the same metric G as in the preceding case. Here the functional $\mathscr{D}^h = 2.17$ is smaller than that of Fig. 11. If to execute the minimizing procedure (24) within a long time, at some moment, due to truncation errors, the symmetry of the problem is broken and the upper boundary nodes begin to go away of the sinusoid peak $z(0,0) = 2$, because it is more "profitable" for the discrete functional. For the mesh depicted in Fig. 13, the functional is $\mathscr{D}^h = 1.67$. In the vicinity of the corner (sinusoid peak), the coordinate surfaces behave likewise in 2D

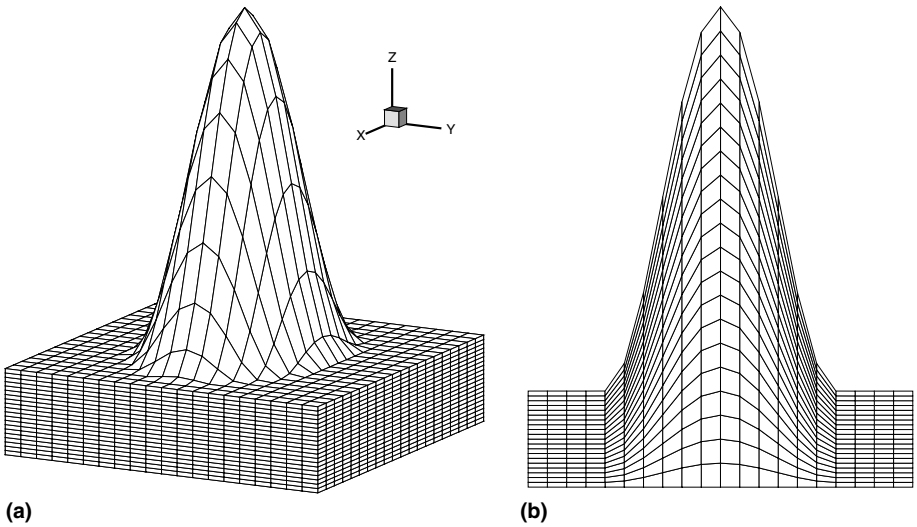

Fig. 9. Initial $21 \times 21 \times 21$ mesh on the bounding surface (a) and coordinate surface $i = 11$ in the plane of symmetry $x = 0$ (b). Transfinite interpolation is applied.

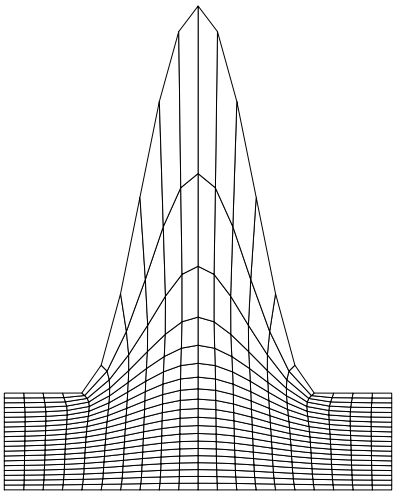

Fig. 10. Mesh generated with the Euclidian metric G.

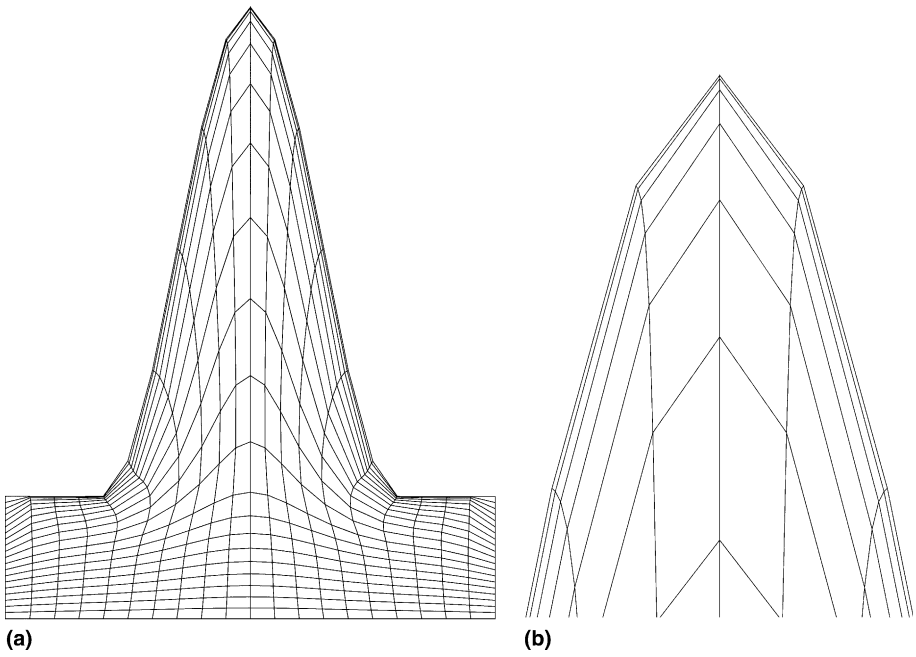

Fig. 11. Mesh condensing towards the upper boundary. Mesh (a) and close-up (b).

when constructing a conformal mapping. In [44], for the model example of the conformal mapping, it was demonstrated and explained why the grid lines attract to the concave zone of the boundary and repel of the convex part. In Section 9, it is noted that in 2D the constrained minimization produces a conformal transformation. Thus, the algorithm of moving the boundary nodes should be applied carefully. Sometimes the iterative procedure should not achieve convergence. To redistribute the boundary nodes, it is sufficient to execute several tens iterations of the minimization procedure and further one should fix them. To avoid an undesirable scattering of nodes shown in Fig. 13, one may define properly the metric G. As noted in Section 3, if to define G equal g taken from the preceding stage of calculation, then the grid will not change. Further G is corrected in a manner so as to improve the grid cell shape. To this end in [35,36] for 2D calculations, it is suggested to employ the correcting functionals. One should note that the correcting functionals may lose invariance to the transformations of the coordinates specified in Section 2.

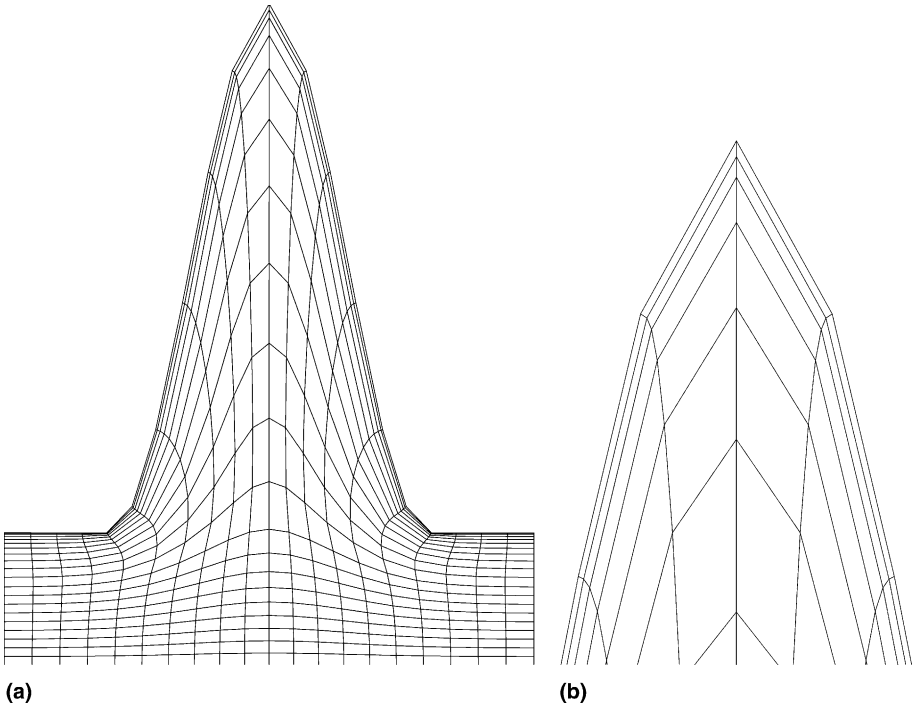

Fig. 12. Mesh condensing and boundary nodes redistribution. Mesh (a) and close-up (b).

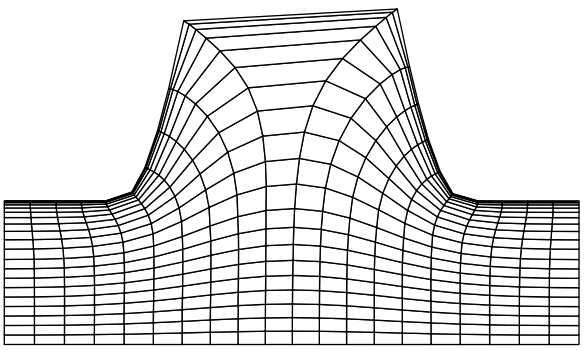

Fig. 13. The same in rather large number of iterations.

Finally, in the example shown in Fig. 14, the mesh is condensed and orthogonalized towards the upper boundary. The domain, where the ζ lines are orthogonal to the upper boundary, consists of five cell layers. The ratio of the parameter Δl in (27) in the first cell layer to Δl in the fifth cell layer is equal to 0.1 and in the fifth cell layer $\Delta l = 0.01$. Afterward, within the 10 transition layers the metric G transforms to Euclidian. The nodes move on the all bounding surfaces and edges except the upper boundary, i.e., surface $k = 21$. It is important to note that some dodecahedral cells near the upper boundary have one inverted internal tetrahedron (T_{2457} or T_{1368}, see Fig. 2(b) and (c)). That is why for this mesh the functional is discretized only on the 8 corner tetrahedra. The analogous event is observed for the initial mesh in Fig. 9 if to define $G = g$. Note that one could refine the mesh on the boundary in such a subdomain so as to avoid over-twisting of the hexahedral cells and then the internal tetrahedrons will not be inverted. The functional minimum is $\mathscr{D}^h_{\min} = 1.58$. In Fig. 14, it is seen that the grid lines bend sharply while passing from the last boundary cell layer to the transition cell layer. This bend can be smoothed, see Fig. 15. Here, in the first three upper layers, the grid lines are orthogonal to the boundary (more precisely to the correspondent coordinate surface), next from the fourth

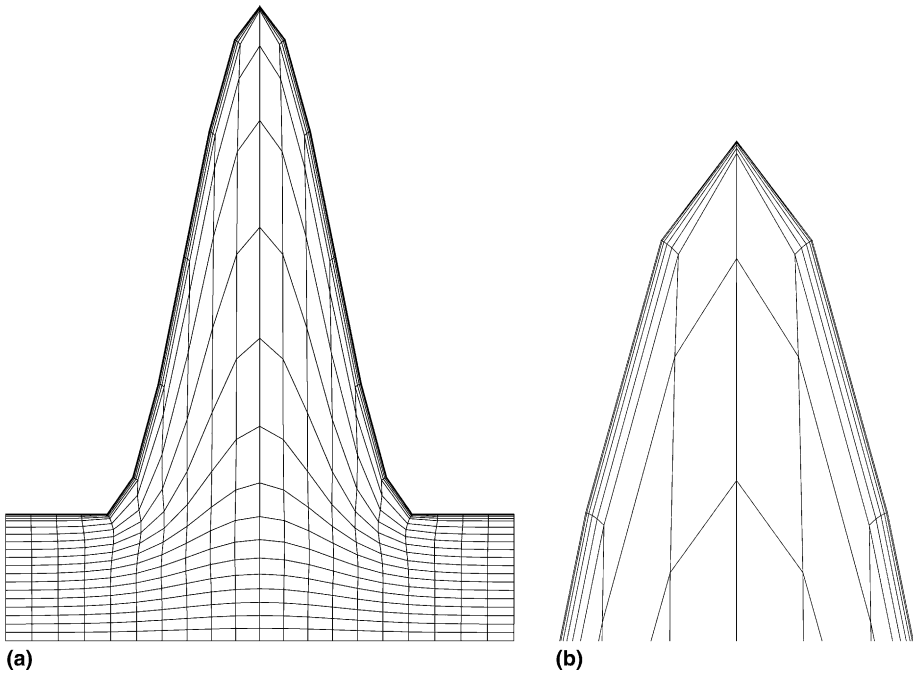

Fig. 14. Mesh condensing and orthogonalization. Mesh (a) and close-up (b).

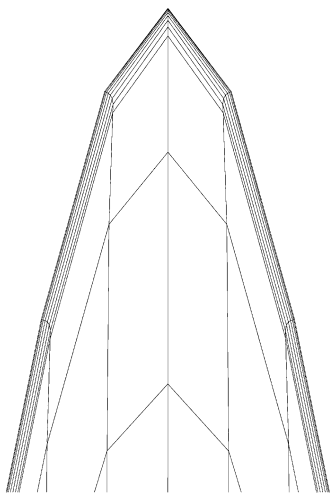

Fig. 15. The same plus smoothing the bend. Close-up.

to seventh layer the ζ line inclination changes linearly to the inclination of the correspondent edge in the eighth cell layer. The transition layer consists of the 8 cell layers and in the remaining five layers the metric G is Euclidian. For this mesh $\mathscr{D}^h_{\min} = 1.44$. Note that $\mathscr{D}^h_{\min}$ for the quasi-uniform mesh, see Fig. 10, is greater than that for the mesh of Figs. 14 and 15. This is because for the latter in the boundary cell layer the integrand E is close to the minimum equal 1, meanwhile for the former, where G is Euclidian, the grid near the upper boundary is far from the cubic mesh where the absolute minimum is attained. In all above cases the check of the hexahedral cells for non-degeneracy has shown that they are non-folded. The computer code, executing this check, includes the verification of the both sufficient and necessary conditions of cell non-degeneracy

dly provided by Us
periment of Section 4

f turbine channel

h is generated in the i
indly provided by Kote

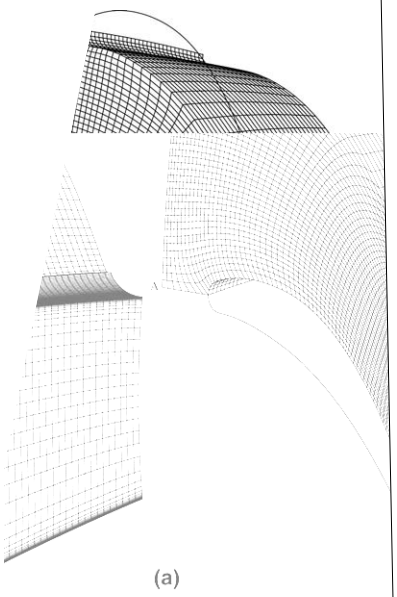

1×31 mesh on the bounding surface. Quasi-u

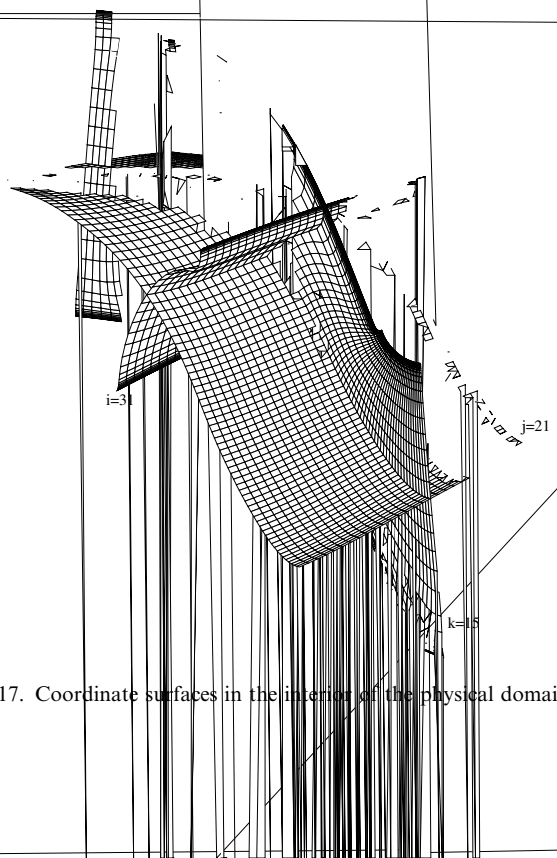

Fig. 17. Coordinate surfaces in the interior of the physical domain.

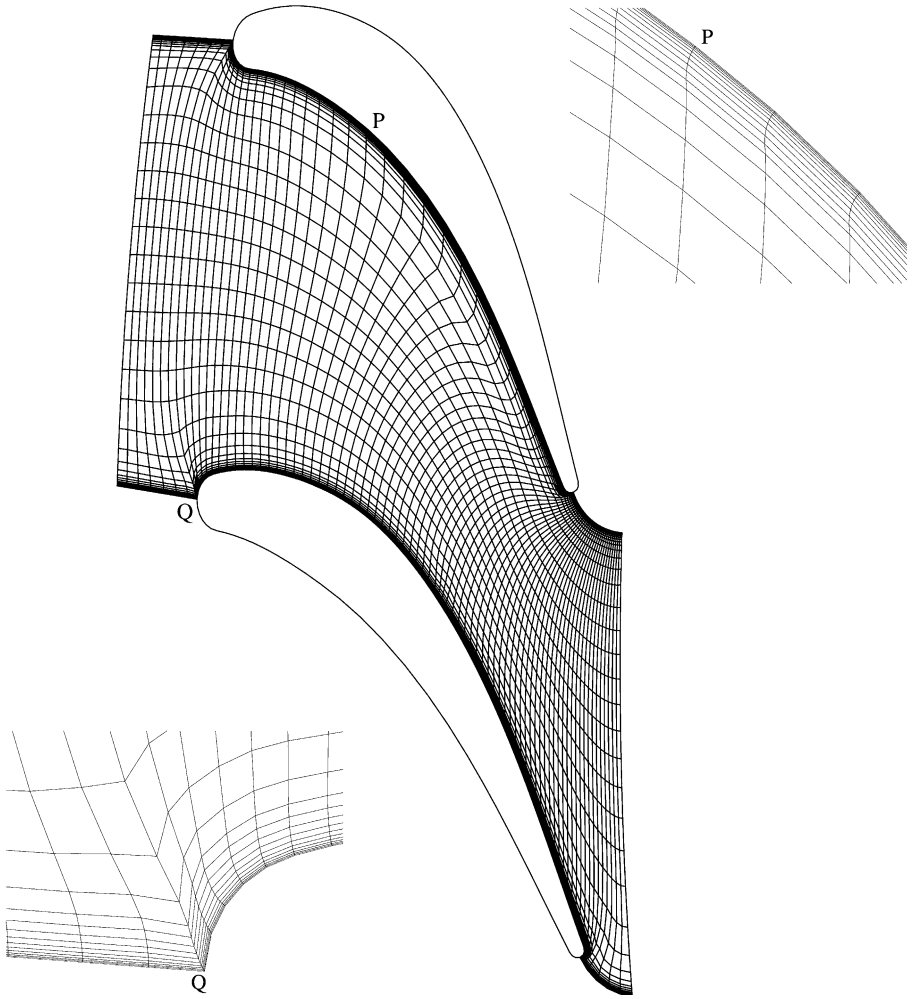

Fig. 18. Bounding surface $k = 31$ and close-up in the vicinity of the points P and Q.

metric G, is shown in Fig. 16(a). The boundary nodes move on the four bounding surfaces $i = 1, 81$, $k = 1, 31$ and four corresponding bounding edges. The bounding surface of the physical domain is a union of ruled surfaces given by the set of supporting points. Each ruled surface is given by four vertices in space. The boundary nodes move on these surfaces. The nodes on the coordinate surfaces $j = 1, 41$ (they contain the blade surfaces) are fixed. The functional is discretized on the 10 basic tetrahedra. The mesh generated with grid lines orthogonalization and impaction towards the blades is presented in Figs. 16(b) and 17. In Fig. 18, the bounding surface $k = 31$ (indicated by the points A, B, C, and D in Fig. 16(a)) is shown. There are the 10 boundary cell layers and 5 transition layers. The ratio of the parameter Δl in the 1st layer to Δl in the 10th layer is equal to 0.1. For the quasi-uniform mesh $\mathscr{D}^h_{\min} = 2.09$ and for the orthogonalized one $\mathscr{D}^h_{\min} = 1.29$.

13. Other functionals

The functional (7) is not the only possible. An arbitrary function $\varphi(E)$, increasing monotonically when $E \geqslant 1$ (for instance, a power function $\varphi(E) = E^{\alpha}$, $\alpha > 0$), also enables to produce an arbitrary given mesh with the metric G properly defined. If the absolute minimum of the functional (7) is attained, for another functional, constructed via $\varphi(E)$, the absolute minimum is attained on the same mesh. If the absolute minimum of (7) is not attained, minimizing another functional produces another mesh.

When constructing the function (3) in 3D we did not use one more invariant of the metric h

$$I_2 = \sum_{i=1}^{3} \text{cofactor } h_{ii} = \det(G^{-1}g)\mathrm{tr}((G^{-1}g)^{-1}) = \frac{\det g}{\det G}\mathrm{tr}(g^{-1}G).$$

In [11,12], the functional depending on the ratio I_{n-1}/I_n are called the functional of smoothness. In [10,30], it was employed a dimensional functional of this kind. However, rather an important property of the functional is invariance to coordinate axes dilatation. That is why the functional should be non-dimensional. Consider a non-dimensional ratio of the invariants abiding by [12] (p. 311)

$$\left(\frac{I_{n-1}}{I_n^{1-1/n}}\right)^{\alpha}, \quad \alpha > 0.$$

With $n = 3$ substituting the expressions for the invariants I_2, I_3 we obtain

$$\left(\frac{I_2}{I_3^{2/3}}\right)^{\alpha} = \left(\frac{\det g}{\det G}\mathrm{tr}(g^{-1}G)/(\det(G^{-1}g))^{2/3}\right)^{\alpha} = \left(\left(\frac{\det g}{\det G}\right)^{1/3}\mathrm{tr}(g^{-1}G)\right)^{\alpha}. \tag{29}$$

Note, the presence of the Jacobian in the denominator of the function (3) plays the fundamental role. When discretizing the functional (7), owing to J in the denominator, the difference function $\mathscr{D}^h$ possesses the barrier property which allows to generate non-folded meshes. The absence of J (or $\det g$ raised to some power) in the denominator of (29) may cause some difficulties when using the invariant I_2 to I_3 ratio. It concerns, at least, domains of complicated geometry.

14. Conclusion

A variational method of the structured grid generation based on minimizing the functional is considered. For every cell the functional is approximated on the 10 tetrahedra forming two dodecahedral cells. The non-degeneracy condition for a hexahedral cell is replaced by the non-degeneracy condition for the above 10 tetrahedra which is the check of the sign of the algebraic volume. The discrete functional possesses an infinite barrier on the boundary of the set of non-folded dodecahedral cells that ensures generation of the non-folded mesh composed of such cells. In the most practical applications the hexahedral grid with the same nodes is also non-folded. The use of the control metric allows to generate an arbitrary given non-folded mesh and, in particular, to involve a supplementary governing for the cell shape and generate an orthogonal mesh with condensed coordinate surfaces towards the boundary. The algorithm of the boundary node redistribution is suggested. The present method can be extended to the unstructured mesh generation in the straightforward manner.

Acknowledgements

The author thanks Olga Ushakova, Institute of Mathematics and Mechanics, Ekaterinburg, with whom Section 4 was coordinated, for fruitful discussions and providing the computer code of testing grid non-degeneracy. This work was partially supported by the Department of Mathematical Sciences of the Russian Academy of Sciences (Program No. 3).

References

[1] A.F. Sidorov, On one algorithm for computing optimal difference grids, Proc. Steklov Math. Inst. 24 (1966) 147–151.
[2] A. Winslow, Numerical solution of the quasi-linear Poisson equation in a nonuniform triangle mesh, J. Comput. Phys. 1 (1966) 149–172.
[3] S.K. Godunov, G.P. Prokopov, On computation of conformal transformations and construction of difference meshes, USSR Comput. Math. Math. Phys. 7 (1967) 209.
[4] S.K. Godunov, G.P. Prokopov, The use of moving meshes in gas-dynamics calculations, USSR Comput. Math. Math. Phys. 12 (1972) 182.
[5] P.P. Belinskii, S.K. Godunov, Yu.B. Ivanov, I.K. Yanenko, The use of a class of quasiconformal mappings to construct difference grids in domains with curvilinear boundaries, USSR Comput. Math. Math. Phys. 15 (6) (1975) 131–139.
[6] J.U. Brackbill, J.S. Saltzman, Adaptive zoning for singular problems in two dimensions, J. Comput. Phys. 46 (1982) 342–368.

[7] J.F. Thompson, Z.U.A. Warsi, C.W. Mastin, Numerical Grid Generation, North-Holland, New York, 1985.
[8] O.-P. Jaquotte, A mechanical model for a new grid generation method in computational fluid dynamics, Comp. Meth. Appl. Mech. Eng. 66 (6) (1988) 323–338.
[9] S.A. Ivanenko, A.A. Charakhch'yan, Curvilinear grids of convex quadrilaterals, USSR Comput. Math. Math. Phys. 28 (2) (1988) 126–133.
[10] S.A. Ivanenko, Adaptive-Harmonic Grid Generation, Computing Center of Russian Academy of Sciences, Moscow, 1997.
[11] V.D. Liseikin, On generation of regular grids on *n*-dimensional surfaces, USSR Comput. Math. Math. Phys. 31 (11) (1991) 47–57.
[12] V.D. Liseikin, Grid Generation Methods, Springer-Verlag, New York, 1999.
[13] P. Knupp, S. Steinberg, Fundamentals of Grid Generation, CRC Press, Boca Raton, FL, 1993.
[14] J.F. Thompson, B.K. Soni, N.P. Weatherill (Eds.), Handbook of Grid Generation, CRC Press, Boca Raton, FL, 1999.
[15] S.A. Ivanenko, Selected Chapters on Grid Generation and Applications, Dorodnicyn Computing Centre of Russian Academy of Sciences, Moscow, 2004.
[16] O.V. Ushakova (Ed.), Advances in Grid Generation, Nova Science Publishers, New York, 2005.
[17] T.I. Serezhnikova, A.F. Sidorov, O.V. Ushakova, On one method of construction of optimal curvilinear grids and its applications, Sov. J. Numer. Anal. Math. Model. 4 (2) (1989) 137–155.
[18] S.K. Godunov, V.T. Zhukov, O.V. Feodoritova, An algorithm for construction of quasi-isometric grids in curvilinear quadrangular regions, in: Proceedings of the 16th International Conference on Numerical Methods in Fluid Dynamics, Arcachon, France, July 6–10, 1998, pp. 49–54.
[19] S.K. Godunov, V.T. Zhukov, O.V. Feodoritova, On one class of quasi-isometric grids, in: O.V. Ushakova (Ed.), Advances in Grid Generation, Nova Science Publishers, New York, 2005 (Chapter 2).
[20] S.P. Spekreijse, Elliptic generation systems, in: J.F. Thompson, B.K. Soni, N.P. Weatherill (Eds.), Handbook of Grid Generation, CRC Press, Boca Raton, Fl, 1999 (Chapter 4).
[21] S.A. Ivanenko, Control of cell shape in the construction of a grid, Comput. Math. Math. Phys. 40 (11) (2000) 1596–1616.
[22] S.A. Ivanenko, B.N. Azarenok, Grid optimization and adaptation, in: O.V. Ushakova (Ed.), Advances in Grid Generation, Nova Science Publishers, New York, 2005 (Chapter 4).
[23] R. Schoen, S.T. Yau, On univalent harmonic maps between surfaces, Invent. Math. 44 (1978) 265–278.
[24] F.T. Farrell, L.E. Jones, Some non-homeomorphic harmonic homotopy equivalences, Bull. Lond. Math. Soc. 28 (1996) 177–182.
[25] N.A. Bobylev, S.A. Ivanenko, I.G. Ismailov, Some remarks on homeomorphisms, Russ. Math. Notes 60 (4) (1996) 593–596.
[26] N.A. Bobylev, S.A. Ivanenko, A.V. Kazunin, Piecewise smooth homeomorphisms of bounded domains and their applications to the theory of grids, Comp. Math. Math. Phys. 43 (6) (2003) 772–781.
[27] S.A. Vavasis, A Bernstein–Bézier sufficient condition for invertibility of polynomial mapping functions, 2003. See <http://www.arxiv.org>, cs.NA/0308021.
[28] O.V. Ushakova, Conditions of nondegeneracy of three-dimensional cells. A formula of a volume of cells, SIAM J. Sci. Comp. 23 (4) (2001) 1273–1289.
[29] O.V. Ushakova, Nondegeneracy conditions for different types of grids, in: O.V. Ushakova (Ed.), Advances in Grid Generation, Nova Science Publishers, New York, 2005 (Chapter 9).
[30] S.A. Ivanenko, Harmonic mappings, in: J.F. Thompson, B.K. Soni, N.P. Weatherill (Eds.), Handbook of Grid Generation, CRC Press, Boca Raton, Fl, 1999 (Chapter 8).
[31] P. Knupp, A method for hexahedral mesh shape optimization, Int. J. Meth. Eng. 58 (2003) 319–332.
[32] T.N. Bronina, I.A. Gasilova, O.V. Ushakova, Algorithms for three-dimensional structured grids generation, Comput. Math. Math. Phys. 43 (6) (2003) 827.
[33] T.N. Bronina, O.V. Ushakova, Application of optimal grid generation algorithms to the volumes of revolution, in: O.V. Ushakova (Ed.), Advances in Grid Generation, Nova Science Publishers, New York, 2005 (Chapter 10).
[34] S.A. Ivanenko, Variational methods for adaptive mesh generation, Comput. Math. Math. Phys. 43 (6) (2003) 793–806.
[35] G.P. Prokopov, Universal variational functionals for 2D grid generation, Preprint of Keldysh Institute for Applied Mathematics of Russian Academy of Sciences, 1, 2001.
[36] G.P. Prokopov, Moving mesh calculation in unsteady two-dimensional problems, in: O.V. Ushakova (Ed.), Advances in Grid Generation, Nova Science Publishers, New York, 2005 (Chapter 5).
[37] V.A. Garanzha, I.E. Kaporin, Regularization of the barrier variational grid generation method, Comp. Math. Math. Phys. 39 (1999) 1426.
[38] P. Knupp, On the invertibility of the isoparametric map, Comp. Meth. Appl. Mech. Eng. 78 (1990) 313–329.
[39] P. Knabner, S. Korotov, G. Summ, Conditions for the invertibility of the isoparametric mapping for hexahedral finite elements, Finite Elem. Anal. Des. 40 (2) (2003) 159–172.
[40] P. Knabner, G. Summ, The invertibility of the isoparametric mapping for pyramidal and prismatic finite elements, Numer. Math. 88 (2001) 661–681.
[41] B.N. Azarenok, Variational barrier method of adaptive grid generation in hyperbolic problems of gas dynamics, SIAM J. Numer. Anal. 40 (2) (2002) 651–682.
[42] P. Knupp, Hexahedral and tetrahedral mesh untangling, Eng. Comput. 17 (3) (2001) 261–268.
[43] J.M. Escobar, G. Montero, R. Montenegro, E. Rodriguez, An algebraic method for smoothing surface triangulations on a local parametric space, Int. J. Numer. Meth. Eng. 66 (4) (2006) 740–760.
[44] G.P. Prokopov, Methodology of variational approach in quasi-orthogonal grid construction, Voprosy Atomnoj Nauki i Techniki (VANT), Ser. Math. Model. Phys. Process. (1) (1998) 37–46.